Palaeogeography, Palaeoclimatology, Palaeoecology 655 (2024) 112542

Contents lists available at ScienceDirect

Palaeogeography, Palaeoclimatology, Palaeoecology

journal homepage: www.elsevier.com/locate/palaeo

Melanoides tuberculata and *Zootecus insularis* gastropod shells provide a snapshot into past hydroclimatic conditions of arid environments: New perspectives from Oman

Katharina E. Schmitt [a,*,1], Tara Beuzen-Waller [b,1,*], Conrad Schmidt [c], Lucas Proctor [d], Susanne Lindauer [e], Christoph J. Gey [a], Dana Pietsch [f], Bernd R. Schöne [a]

[a] Institute of Geosciences, University of Mainz, Johann-Joachim-Becher-Weg 21, 55128 Mainz, Germany
[b] Université de Perpignan, Via Domitia, Histoire Naturelle de l'Homme Préhistorique (HNHP), UMR 7194 CNRS, UPVD 52 avenue Paul-Alduy, 66860 Perpignan, France
[c] Institute for Ancient Near Eastern Studies (IANES), University of Tübingen, Burgsteige 11, 72070 Tübingen, Germany
[d] Institute for Archaeological Sciences, Johann Wolfgang Goethe University, Norbert-Wollheim-Platz 1, Frankfurt amMain, Germany
[e] Curt Engelhorn Center Archaeometry gGmbH, 68159 Mannheim, Germany
[f] Chair of Soil Science and Geomorphology, University of Tübingen, Rümelinstr. 19-23, 72072 Tübingen, Germany

ARTICLE INFO

Editor: Amy Prendergast

Keywords:
Geoarchaeology
Terrestrial snails
Freshwater snails
Sultanate of Oman
Palaeoenvironment

ABSTRACT

Shells of the aquatic gastropod *Melanoides tuberculata* and the terrestrial gastropod *Zootecus insularis* were analysed using high-resolution isotope sampling (up to 274 samples per shell) to assess their potential use as a proxy for hydroclimatic and palaeoenvironmental reconstruction in drylands. A total of 169 snails (fossil and modern) were collected from 37 sites in Northern Oman and Dhofar, with each site selected for its specific geomorphological, archaeological or ecological context. This included fluvial terraces, playa environments, modern oasis gardens, irrigation channels and archaeological sites from the Neolithic (6,000–3,200 BCE) and Early Bronze Age (3,200–2,000 BCE) periods. The $\delta^{18}O$ data obtained from these gastropods could be classified into eight different patterns, three for the aquatic snails (Type 1 A–C) and five for the terrestrial snails (Type 2 A–E), which were linked to the environmental context of their habitat. Furthermore, the use of the aquatic snails enabled us to distinguish between groundwater and surface water signals, whereas the terrestrial snails were employed to reconstruct changes in rainfall origin, humidity, evaporation, regular wet-dry cycles, and meteorological events. According to the results, gastropods can be used to elucidate the long-term, local evolution of rain-fed floodplain ecosystems in drylands and to identify the hydrological resources present in the vicinity of archaeological sites, particularly with regard to type 1 A-C (e.g., surface water vs groundwater).

1. Introduction

Throughout the Quaternary, the climate of Oman was characterised by alternating periods of arid and humid conditions, which have been attributed to fluctuations in the mean latitude of the Intertropical Convergence Zone (ITCZ) over time (Fleitmann et al., 2007). In periods when the ITCZ migrated further southward (e.g., today), summer monsoon precipitation was weakened and only reached as far north as the Dhofar region (Weyhenmeyer et al., 2000). In periods when it moved further northward (e.g., Holocene Humid Period; Fontes et al., 1993; Fig. 1) much of northern Oman received increased mean annual precipitation (Fleitmann et al., 2003). This would have led to the emergence of *khareef*-like conditions (*kharīf* = local Arabic term for the southeastern monsoon from June to early September) characterised by high humidity, moderate temperatures, increased rainfall, and fog throughout the region, transforming the Arabian Desert into verdant landscapes with permanent lakes or wetlands (Rosenberg et al., 2012; Matter et al., 2015; Parker et al., 2016). Such periods have been documented in the Pleistocene and the Holocene (10,500 to 6,000 years ago; Fleitmann et al., 2003, 2007). Wadis benefited from more intense and regular flow (Blechschmidt et al., 2009; Woor et al., 2022) and vegetation density increased (Parker et al., 2004). This has been associated with greater accessibility of local water resources, which is believed to play an important role in the dispersal of hominins both within and

* Corresponding authors.
E-mail addresses: katharina.schmitt@uni-mainz.de (K.E. Schmitt), Tara.Beuzen-Waller@univ-perp.fr (T. Beuzen-Waller).
[1] These authors contributed equally to this work (joint first authorship)

https://doi.org/10.1016/j.palaeo.2024.112542
Received 28 June 2024; Received in revised form 21 August 2024; Accepted 2 October 2024
Available online 8 October 2024

beyond Arabia (Armitage et al., 2011; Parton et al., 2015; Breeze et al., 2016). Furthermore, it has been postulated that they may have influenced the settlement patterns during the Holocene in Oman, particularly during the Neolithic (6,000–3,200 BCE) and the Early Bronze Age (3,200–2,000 BCE) (Preston et al., 2015).

In contrast, dry periods are characterised by infrequent and spatially limited rainfall (coastal areas: 60–100 mm/yr; mountainous regions: 200–300 mm/yr) with a high inter-annual variability driven by the Westerlies and the Mediterranean depression (Weyhenmeyer et al., 2002), which makes Oman exposed to chronic water stress. Meteorological events such as cyclones originating from the Indian Ocean can also contribute to rainfall. The southern coast of Oman is exposed to cyclones every 5 to 7 years and the northern coast every 10–15 years, but the frequency of those phenomena is escalating with climate change (Mansour et al., 2021). Such events can result in the delivery of a considerable quantity of precipitation in a relatively short period. This has been recently illustrated by the tropical Cyclones Gonu (2007) and Shaheen (2021), which delivered 625 mm (Elgamal et al., 2007) and > 300 mm of precipitation in Muscat (Terry et al., 2022), respectively, in one day. Cyclones are mainly impacting coastal areas but some of them can penetrate inland (for instance Mekunu in 2018) (Andreou et al., 2022).

In Oman, reconstructing the temporal and spatial characteristics of past rainfall and its associated humid or dry periods is complicated by the need to rely on terrestrial archives such as speleothems, lacustrine deposits (Nicholson et al., 2020) and fluvial sediments (Parton et al., 2015; Beuzen-Waller et al., 2022). All of these archives have inherent limitations, including that they are site-specific, require sufficient rainfall to form (Fleitmann et al., 2011; Mueller et al., 2023), can be influenced by groundwater fluctuations, or are discontinuous (Blechschmidt et al., 2009; Hoffmann et al., 2015; Beuzen-Waller et al., 2022; Mueller et al., 2023; Woor et al., 2022). Furthermore, the poor preservation of biomarkers in arid and semi-arid regions, resulting from weathering, drought-induced diagenetic alteration, and deflation, represents a significant challenge to local-scale palaeoenvironmental reconstructions.

Terrestrial and fresh/brackish-water gastropod shells represent hitherto unexploited archives for climate reconstructions in Oman. This is surprising given that these shells can be found in a variety of environments and in many different temporal and spatial contexts (Beuzen-Waller, 2020; Girod and Sassoon, 2022). Following previous studies, stable isotope data ($\delta^{18}O$ and $\delta^{13}C$) of aragonitic shells can be used to reconstruct palaeoenvironmental conditions (e.g., Stott, 2002; Balakrishnan and Yapp, 2004; McConnaughey and Gillikin, 2008; Schöne, 2008; Yanes et al., 2009; Prendergast et al., 2015; Louis et al., 2022; Stringer and Prendergast, 2023). Although most of these studies use bulk samples (providing an average environmental signal recorded over the lifetime of the animal), there are studies that employed higher-resolution sampling to obtain more detailed environmental data (e.g., Leng et al., 1998; Taft et al., 2014, 2020; Zaarur et al., 2016; Ghosh et al., 2017; Long et al., 2020; Dong et al., 2022; Schmitt et al., 2022; Quenu et al., 2023; Li et al., 2024).

In this study, high-resolution sampling with a 0.5 to 1.5 mm spacing (up to 274 samples per shell; for exact number see Supplementary S1) was conducted on 56 specimens of the aquatic (freshwater/brackish-water) gastropod species *Melanoides tuberculata* (O. F. Müller, 1774) and on 113 specimens of the terrestrial species *Zootecus insularis (*Ehrenberg, 1831). A total of 6288 samples were drilled for stable isotope analysis ($\delta^{13}C$ and $\delta^{18}O$), with which we evaluated the potential of the snail shell as an insight into past hydroclimatic and palaeoenvironmental conditions in drylands. The shells originated from specific geomorphological contexts including channel deposits, overbank deposits as well as playa depressions (Fig. 3). Additionally, archaeological contexts were considered including sites from the Neolithic period (approx. 6,000–3,200 BCE, during the Holocene Humid Period) and from the Early Bronze Age (approx. 3,200–2,000 BCE, starting at the onset of arid conditions). Shells from modern contexts, sampled in karstic springs, oasis gardens and *falaj* irrigation canals (underground galleries draining groundwater until it reaches the surface, whereupon it is redirected towards villages and agricultural plots), were analysed as modern reference materials (Fig. 2; for coordinates, please see Supplementary S2). The typology of the $\delta^{18}O$ signals was then compared to their stratigraphic, geomorphologic, and archaeological context of sampling to test their accuracy, their capacity to characterise water body types (ephemeral, permanent, subject to evaporation, continuously or discontinuously supplied with water) and to record climatic fluctuations or anthropogenic watering.

2. Material and methods

All data including sections position, full descriptions as well as results from sedimentary and geochemical analyses will be stored in an open access WebGIS (https://www.umweltwandel.online/webgis/). The reader is referred to the Supplementary Data (doi.https://doi.org/10.5281/zenodo.13341949) for detailed information regarding the isotopic data of the snail shells and their position in the stratigraphic profile as well as for the profile description (S3–S39).

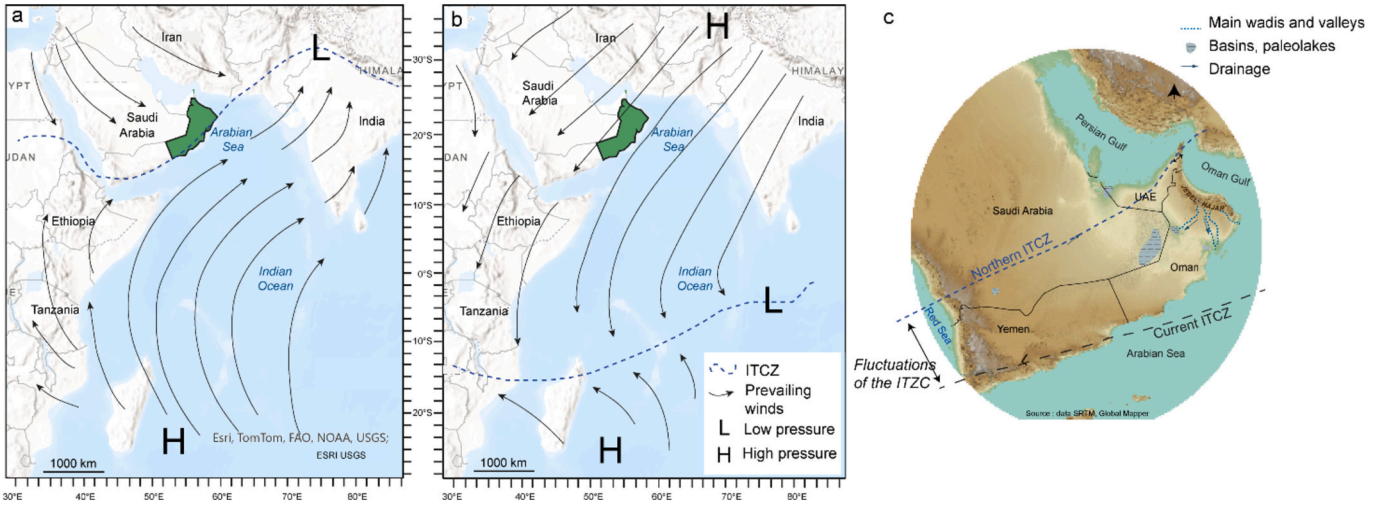

Fig. 1. (a) The Indian Ocean Monsoon system and the current position of the inter-tropical convergence zone (ITCZ) during summer. (b) The Indian Ocean Monsoon system and the current position of the ITCZ during winter, redrawn from Fleitmann and Matter (2009). (c) Suggested northern position of the summer ITZC during humid periods (from Van Rampelbergh et al., 2013).

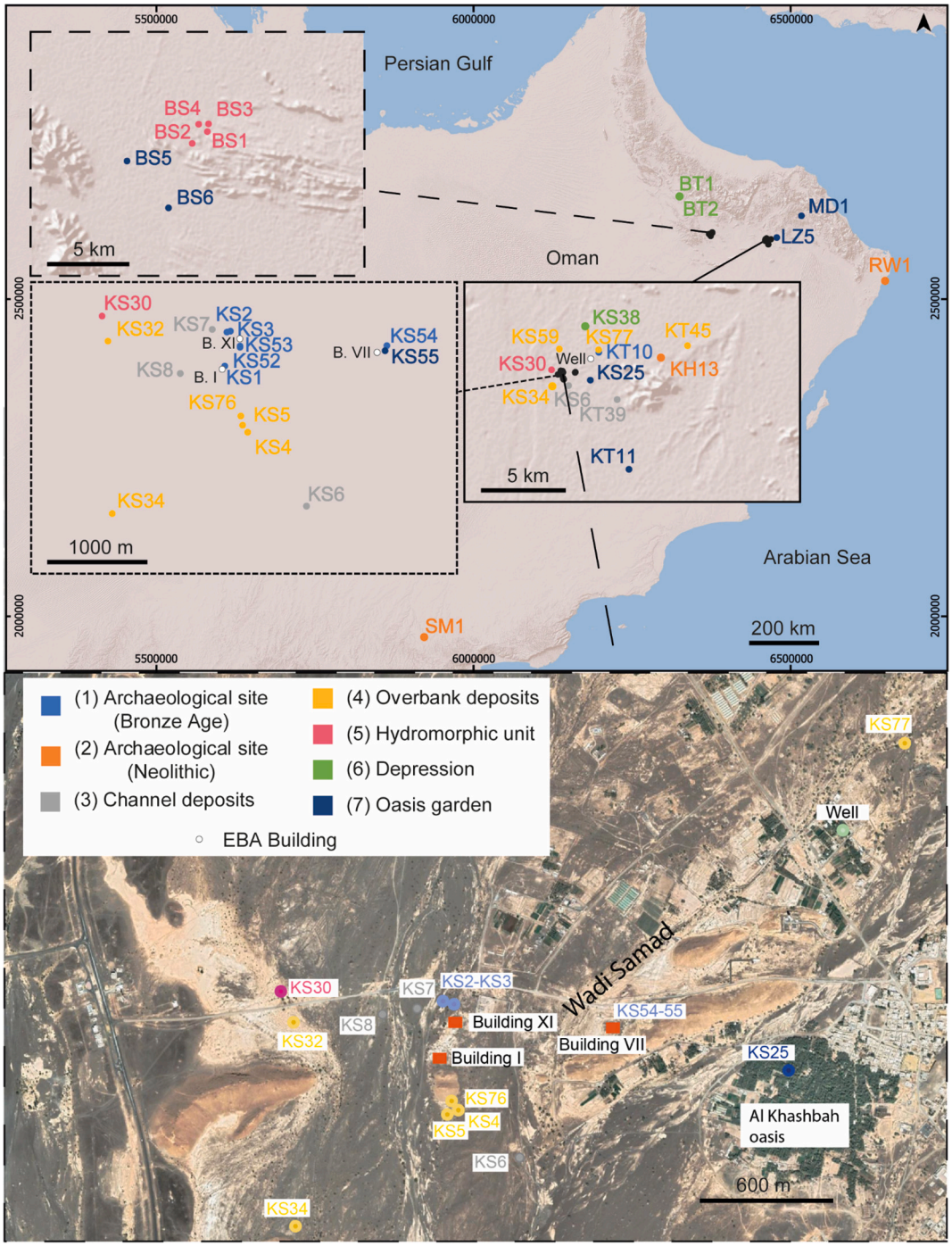

Fig. 2. Geographical overview of the 37 sections analysed in this study. The various geomorphological contexts are depicted in different colours. Early Bronze Age Buildings I, VII and XI (EBA Building: B. I; B VII; BXI) are indicated on both the map and the satellite image. Furthermore, on the satellite image, Wadi Samad and the Al-Khashbah oasis are indicated. Due to the proximity of the individual sections to each other, it has been necessary to enlarge some map sections (dashed lines and frames) in order to facilitate their recognition. (Source: top: Base Map ESRI Shaded Relief, layout Conrad Schmidt, down: Google Earth imagery, caption from 2021, layout Tara Beuzen-Waller).

2.1. Geomorphological and archaeological sampling strategy

The collection of snails was investigated as part of a multidisciplinary project (UmWeltWandel Project; UWW) dedicated to the reconstruction of the environment and settlement during the Neolithic and Bronze Age in Northern Oman. In this context, 37 sections were opened in fluvial terraces with the objective of studying and dating phases of alluvial aggradation in wadi systems during the Holocene. Each section was described and sampled for dating purposes (publication in preparation). The snails were hand-picked from precisely recorded stratigraphic contexts. For a full description of each section and corresponding stratigraphic layers the reader is referred to the Supplementary Data and the WebGIS. The section names consist of two letters and a number (e.g., KS11), and snail sample code started with a U followed by a number (e.g., U2001).

Gastropods examined in this study originated from or within a 100-m radius of Neolithic (2) or Early Bronze Age (1) sites (Fig. 3). All sites are located on a fluvial terrace or near an active wadi system. Neolithic

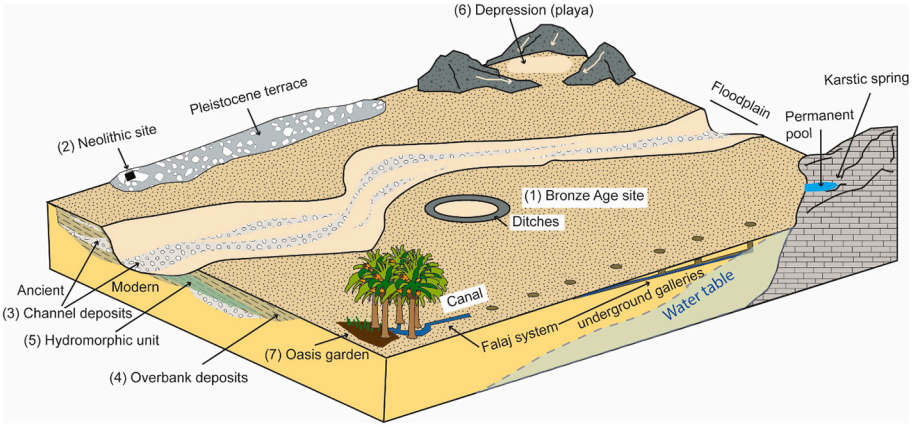

Fig. 3. Schematic illustration of the context of sampling (1) Bronze Age site, including monumental building and circular ditches, (2) Neolithic site, including fireplace and area within a 100 m radius, (3) fossilised channel deposits from a low fluvial terrace, (4) fossilised overbank deposits from a low fluvial terrace, (5) hydromorphic units with in overbanks deposits, (6) depressions and playa sedimentation, and (7) oasis gardens (palm groves) fed by *falaj*.

snails come from excavated archaeological contexts or its surroundings. The gastropods from the Early Bronze Age site were collected from excavations within Early Bronze Age buildings or from specific areas assumed to be linked to early-stage water management activities (such as 'ditches'; Fig. 3). Most shells were collected from the archaeological site complex of Al-Khashbah (UWW project); other specimens selected for comparison came from various different sites (see Table 1).

More snails were collected from low fluvial terraces built up during the early to mid-Holocene. These fluvial deposits consist of three main types: (3) 'channel deposits', characterised by coarse materials consisting of well-rounded pebbles and boulders or heterometric materials in a coarse, sandy matrix and refers to the most active part of the floodplain; (4) 'overbank deposits', defined by fine deposits dominated by sorted fine sands and silt; in some cases these present (5) 'hydromorphic units' in areas affected by the water table or being consistently humid (Fig. 3). Finally, a few samples were collected from (6) local depressions (*playas*). These are small basins that collect run-off water from low elevation hills and are filled with silty to sandy sediments (Fig. 3). To provide a reference for the isotope signal, modern aquatic samples were collected from oasis garden (7), irrigated by a *falaj* canal, or by electrically pumped water. Additionnaly, modern samples were collected in a wadi at the natural outlet of a karstic spring (Dima wa at-Tayyin in Northern Oman) (Fig. 3).

2.2. Sclerochronological sampling strategy

113 adult specimens of the terrestrial snail *Z. insularis* and 56 adult specimens of the aquatic snail *M. tuberculata* were collected from 37 sites. All shells were collected dead except for those from KS25. The selected shells were freed from dirt and debris by mechanical cleaning, then placed in Eppendorf cylinders with deionized water and shaken for 24 h on a shaking table. Subsequently, the specimens were subjected to repeated ultrasonic rinsing before being dried in an oven at 40 °C for 24 h. Then, samples were analysed using Raman spectroscopy (S43) to preclude the presence of any diagenetic alteration before carbonate powders were collected for $\delta^{13}C$ and $\delta^{18}O$ measurements via manual high-resolution micromilling on the shell surface (Fig. 4). Although the isotopes of both oxygen and carbon were measured, this study focused primarily on the oxygen isotopes. For a detailed description of the methodology, please refer to the Supplementary Material (S40). Carbon isotopes were only used as an indicator of diagenetic alteration or to determine measurement errors. All sampled shells were sent to the Curt-Engelhorn-Zentrum Archäometrie gGmbH in Mannheim for ^{14}C dating (see S41).

2.2.1. Melanoides tuberculata

The aquatic snail, *M. tuberculata*, secretes its aragonitic shell from the extrapallial fluid in isotopic equilibrium with the surrounding water (Abell, 1985; Leng et al., 1999; Kieniewicz and Smith, 2007; Shanahan et al., 2005). This species is primarily found in standing or slow-moving water (De Kock and Wolmarans, 2009), on rocky or muddy substrate at depth > 20 cm to 2 m (Shanahan et al., 2005) in freshwater habitats but can also tolerate brackish water (De Kock and Wolmarans, 2009; Raw et al., 2016; Leng et al., 1999), which is only the case for site RW1 in this sample set. To reconstruct palaeotemperature, the Grossman and Ku (1986) palaeothermometry equation was used with the VPDB-VSMOW scale correction of -0.27 ‰ (cf. Gonfiantini et al., 1995; Dettman et al., 1999) and a $\delta^{18}O_{water}$ value of -1.17 ‰ (see S42). This value represents the arithmetic mean of data from a well in Al-Khashbah (coordinates: UTM-WGS84: 40Q 606980.844E 2506633.639N; Fig. 2), which were obtained during fieldwork campaigns 2022 and 2023:

$$T_{\delta^{18}O}[^{\circ}C] = 20.60 - 4.34 \times \left(\delta^{18}O_{shell} - \left(\delta^{18}O_{water} - 0.27\right)\right) \quad (1)$$

To ascertain whether the aquatic environment was fed by groundwater or rainwater, the stable oxygen isotope signature of water ($\delta^{18}O_{water}$) was reconstructed from $\delta^{18}O_{shell}$ data using eq. (1), solved for $\delta^{18}O_{water}$ (Schöne et al., 2020):

$$\delta^{18}O_{water} = \frac{19.43 - 4.34 \times \delta^{18}O_{shell} - T[^{\circ}C]}{-4.34} \quad (2)$$

with $T = 35.72$ °C, the mean annual temperature recorded by a HOBO data logger placed in the aforementioned well (see S42). Oxygen isotope data were presented in δ-notation relative to the Vienna Pee Dee Belemnite (VPDB) while the $\delta^{18}O_{water}$ data were presented in δ-notation relative to the Vienna Standard Mean Ocean Water (VSMOW). A total of 56 shells of *M. tuberculata* were analysed, with samples taken from the aperture to the 3rd–4th whorl. The number of samples taken per shell was dependent on its size, within the range of 4 to 274 intra-annual samples per shell. They all dated to Neolithic and Early Bronze Age. The snails from LZ5, MD1, BS5, BS6 and KS25 are recent and were used as reference material.

2.2.2. Zootecus insularis

Terrestrial snails typically only secrete their aragonitic shell for a few hours per night (Balakrishnan and Yapp, 2004; Balakrishnan et al., 2005) and only within a specific temperature range (Lécuyer et al., 2020). Because of this, temperature was not calculated for this species. *Z. insularis* have been found in Oman in a variety of environments, including agricultural fields, under shady trees, small thick bushes, banks of shady canals, sewage ponds (Qamar et al., 2017), mountain

Table 1
Context of samples with site (section name), sample number of the aquatic (*Melanoides tuberculata*) and terrestrial (*Zootecus insularis*) snails and origin of the material (either project, archaeological mission or collaborator). Most snails were collected at the archaeological site complex of Al-Khashbah (UWW project); other specimens came from various different sites. The site SM1 is from the surrounding of the Neolithic site of Wadi Stum in Dhofar (EORK project, directed by Maria Pia Maiorano); RW1 refers to the Neolithic site of BJD-1 near Al-Haddah (courtesy of Vincent Charpentier and the Arabian seashore project); KH13 is the code for the Neolithic site of KSH-A in Al-Khashbah (excavated by Maria Pia Maiorano and Lucas Proctor); BT1 and BT2 were collected near the Early Bronze Age site of Rakhat al Madrh, near Bat (excavated by the Bat Archaeological project by Jennifer Swerida and Eli Dollarhide). BS1, BS2, BS3 were obtained from near the Early Bronze Age site of AD-1, AD-2 and AD-3 in Bisya (excavated by the French Archaeological Mission in Central Oman, directed by Mathilde Jean and Martin Sauvage).

Site	Sample no. *Melanoides tuberculata*	Sample no. *Zootecus insularis*	Project and archaeological mission/collaborator
(1) Archaeological site (inside or near an Early Bronze Age)			
KS1	U167	U158; U161	UmWeltWandel (UWW)
KS2	U533	U84; U532	UWW
KS3		U28; U29; U30; U33; U576	UWW
KS52	U898	U896; U903	UWW
KS53		U916; U918; U919; U921; U956-Z; U1043-Z; U1473-FS2-Z; U2203-Z; U2331-Z; U2337-Z; U2509; U2510; U2511; U2512; U2513; U2514; U2515; U2516; U2517; U2518; U2519; U2520; U2521	UWW
KS54	U956-M; U1043-M; U1473-FS1-M; U1473-FS2-M; U2203-M; U2331-M; U2335; U2337-M		UWW
KT10		U2194; U2199; U2200	
(2) Archaeological site (inside or near a Neolithic site)			
KH13	U2532	U2530; U2531; U2533; U2534; U2541	Maria Pia Maiorano, Lucas Proctor
RW1	U3076; U3077; U3078		Vincent Charpentier
SM1	U3051; U3046; U3047; U3048; U3049; U3050	U3039	EORK project: Maria Pia Maiorano
(3) Mid-Late Holocene Channel deposits			
KS6	U4; U7; U13; U8	U503	UWW
KS7		U501	UWW
KS8		U566; U569	UWW
KT39	U2278		UWW
(4) Early-Mid-Late Holocene Overbank deposits			
KS4	U23	U17; U19; U37; U36; U35	UWW
KS5		U38; U39; U40; U74; U80; U2186; U2188; U2189	UWW
KS32	U749	U750	UWW
KS34		U801; U1456; U1457	UWW
KS59		U1165	UWW
KS76		U1955; U1957; U1961; U1963	UWW
KS77		U1966; U1967; U1968; U1969; U1970; U2338	UWW
KT45		U2277	UWW
(5) Early-Mid-Late Holocene Hydromorphic unit			
BS1	U2525; U2526; U2524	U2527; U2528	French Archaeological Mission: Mathilde Jean, Martin Sauvage
BS2	U3041		See BS1
BS3		U3060; U3042	See BS1
BS4	U3043; U3061; U3062		See BS1
KS30	U1451	U728; U729; U1453	UWW
(6) Mid-Late Holocene Depression			
BT1	U3054	U3040; U3052; U3053; U3055; U3057; U3059; U3056; U3058	Bat Archaeological project: Jennifer Swerida, Eli Dollarhide
BT2		U3071; U3072; U3073; U3074; U3075	see BT1
KS38		U834; U1458; U1459	UWW
(7) Modern Garden or Suspected Protohistoric Garden			
BS5	U3044; U3063		UWW
BS6		U3045; U3064; U3065; U3066; U3067; U3068	UWW
KS25	U3069; U3070; U3117		UWW
KS55	U1044; U1048; U1049; U1058; U1064; U1067; U1461-M; U1483-FS8	U1047; U1069; U1466-Z; U1482-Z; U1050	UWW
KT11	U2339-M	U2204; U2207; U2339-Z	UWW
LZ5	U332; U345		UWW
MD1	U1972; U2522; U2523		UWW

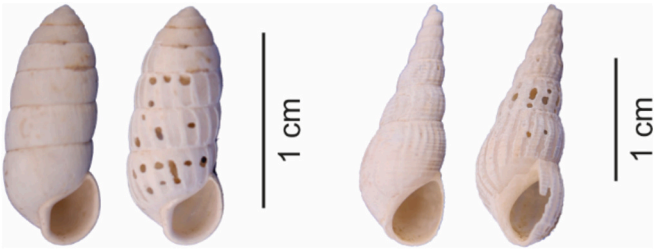

Fig. 4. *Z. insularis* (left) *and M. tuberculata* (right) before and after high-resolution sampling.

environments (up to 1,900 m above sea level), premontane environments (Feulner and Green, 2003), narrow coastal plains, silty soils between rocks, vegetation on mountain slopes, suburban lawns and gardens (Girod and Sassoon, 2022), parks and agricultural fields (Al-Khayat, 2010). They prefer moist soil with a moderate amount of humus (Qamar et al., 2017) and dig to a depth of 25 cm (Al-Khayat, 2010). In total 69 shells of *Z. insularis* of varying ages and sizes were analysed, with 2 to 100 intra-annual samples per shell. The remaining 44 snails were too brittle for high-resolution analysis so that only two to six samples were obtained per specimen. Consequently, these were precluded from further interpretation, although their values were still used as a bulk signal and for dating. All shells dated to the Neolithic and Early Bronze Age, with one exception from KS6 (U503; 659–605 cal BCE). *Z. insularis* was not found in a modern environment or in living position, so no comparative modern reference material is available for the terrestrial dataset.

3. Results

3.1. Isotope signal $\delta^{18}O_{shell}$

The $\delta^{18}O_{shell}$ data were plotted against distance from the aperture (e.g., Fig. 4) in order to identify shifts recorded in the gastropod shells that were caused by changes of environmental conditions. These changes may have been caused by variations in water temperature, water sources, freshwater input, evaporation, and other factors. Upon analysis of the aforementioned graphs, it became evident that the 125 snails could be classified into eight distinct groups, each exhibiting a unique isotopic pattern. The 56 aquatic *M. tuberculata* snails (Type 1) were classified into three distinct pattern types, while the 69 terrestrial *Z. insularis* snails (Type 2) were divided into five types. These patterns were compared visually due to varying lengths, non-uniform sampling intervals, and the presence of non-linear trends and abrupt changes. These factors complicate direct mathematical comparisons, making visual inspection a flexible and effective approach to identify significant patterns and anomalies.

3.1.1. Type 1 A: $\delta^{18}O_{shell}$ variation less than 1 ‰

The $\delta^{18}O_{shell}$ pattern recorded by *M. tuberculata* snails in this category showed overall **variability of less than 1 ‰,** as evidenced by a recent specimen of the snail U3063, which originated from a modern irrigation canal (BS5) (Fig. 5). Another sixteen shells collected from three modern and seven archaeological sites (Table 2) exhibited a similar pattern. Modern sites included a recently abandoned oasis garden (LZ5, BS5) and a wadi fed by a karst spring (MD1). The archaeological sites included Bronze Age ditches close to Building I and XI (KS1, KS52; Fig. 2) and three areas (KS2, KS54, KS55, KT11) close to Early Bronze Age buildings where landscape modification (such as irrigation, gardening, soil improvement) is suspected. BS4 came from a hydromorphic unit. Although the specimens had a comparable degree of intra-shell variation, values of the single shells exhibited considerable variability (Table 2). Temperature variations were calculated using eq. (1), ranging from a minimum of 19.7–22.3 °C (KT11; U 2339-M) to a maximum of 31.5–33.0 °C (KS52; U898). Temperature fluctuations recorded by these shells are limited to a maximum of 4 °C. The carbon isotope values ranged between -16.5 ‰ (U2523) and -7.1 ‰ (U533).

3.1.2. Type 1 B: $\delta^{18}O_{shell}$ variation between 1 and 2 ‰

All 23 *M. tuberculata* snails in this category had a **variability of 1 and 2 ‰ in their $\delta^{18}O_{shell}$ values**, comparable to that observed in the recent aquatic snail U2522 (Fig. 6), which was collected in one inlet of the *falaj* of Al-Khashbah (KS25). In some parts, the isotope values of these snails also exhibited a consistent and gradual increase (e.g., U2522: 0.9 ‰; 14 to 6 mm) or decrease (e.g., U2522: -1.5 ‰; 43 to 35 mm) in certain parts. The snails were collected from modern and archaeological sites (Table 3). This included areas surrounding a Neolithic site in Dhofar (SM1) and Early Bronze Age sites of Bat (BT1), Bisya (BS1, BS4), and Al-Khashbah (KS54 and KS55) (Fig. 2). Modern reference snails were also included, such as KS25 (canal in the oasis of Al-Khashbah). Although the snails recorded a similar $\delta^{18}O_{shell}$ range, the individual range was highly variable (Table 3). The temperature fluctuations calculated from individual shells were constrained to a maximum of 8.6 °C, as determined by eq. (1). The temperature range from all snails was between (min) 16.3–21.4 °C (KS32; U749) and (max) 38.1–45.3 °C (SM1; U3051). The carbon isotope values ranged between -17.2 ‰ (U2523) and -3.8 ‰ (U533).

3.1.3. Type 1 C: $\delta^{18}O_{shell}$ variation greater than 2 ‰

The *M. tuberculata* specimens in this category displayed a notable degree of variability in **their $\delta^{18}O_{shell}$ values, with a range exceeding 2 ‰** (Fig. 7). The maximum observed range was 7.2 ‰ (RW1: U3077). A total of 16 specimens were collected from a variety of archaeological sites, including those dating to the Neolithic (SM1, KH13 and RW1) and the Bronze Age (KS54), as well as an overbank deposit (KS4) and hydromorphic units (BS1 and KS30). The maximum temperature range of a snail from this category was calculated to be 31.2 °C (RW1: U3077), with a range between 15.8 and 45.7 °C (Table 4). The lowest temperature was recorded by specimen U13 (KS6), with a reading of 4.7 °C, while the highest temperature was observed in specimen U3048 (SM1), at 57.0 °C. The carbon isotope values of all snails ranged between -10.4 ‰ (U13) and -2.2 ‰ (U3076).

3.1.4. Type 2 A: Slowly but steadily increasing $\delta^{18}O_{shell}$ values

Nine shells of *Z. insularis* showed **steadily increasing $\delta^{18}O_{shell}$ values** (Fig. 8). These shells were collected from seven different sites (Table 5), with the majority originating from a small depression with playa-sediment infilling (BT1, BT2) or overbank deposits (KS34, KS32, KS4, KT45). One shell was collected from an oasis garden (KT11). The isotope ranges of the single shells exhibited considerable variability, with values spanning from 1.8 ‰ (U3057) to 11.4 ‰ (U2277). Carbon isotope values varied between -11.1 ‰ (U2204) and 0.1 ‰ (U3053).

3.1.5. Type 2 B: Steadily decreasing $\delta^{18}O_{shell}$ values

Six shells of *Z. insularis* showed **steadily decreasing $\delta^{18}O_{shell}$ values** (Fig. 9). They were collected from four different sites (Table 6). Shells from two areas were associated with the Al-Khashbah Early Bronze Age site (KS53 and KS54), while BT1 came from a depression and BS1 from a hydromorphic unit, near Bat and Bisya, respectively. Individual isotope ranges were highly variable, fluctuating between a range of 2.7 ‰ (U1473-FS2-Z) and 12.4 ‰ (U2337-Z; Fig. 9). Carbon isotope values varied between -10.0 ‰ (U2204) and 1.7 ‰ (U3053).

3.1.6. Type 2 C: Sharply dropping $\delta^{18}O_{shell}$ values

Eighteen shells recorded **sharp (and sudden) $\delta^{18}O_{shell}$ drops** (Fig. 10: 27–24 and 20–19 mm). After reaching the most negative point, the $\delta^{18}O_{shell}$ values slowly increased again (Fig. 10: 19-–5 mm). The snails were collected from thirteen different sites, including all environmental contexts (Table 7). Carbon isotope values varied between -10.9 ‰ (U503) and 1.6 ‰ (U84).

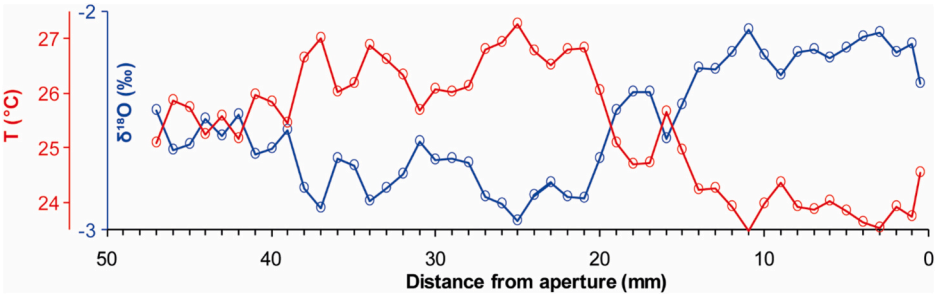

Fig. 5. Stable oxygen isotope data of a *M. tuberculata* snail U3063 (blue) along with reconstructed water temperatures (red). (For interpretation of the references to colour in this figure legend, the reader is referred to the web version of this article.)

Table 2
Summary of snails with a $\delta^{18}O_{shell}$ variability of <1 ‰. The species (sp.: *M. tub.* = *Melanoides tuberculata*), sample name, section (sec), measured $\delta^{13}C_{shell}$ and $\delta^{18}O_{shell}$ range (min and max) and calculated mean (Ø) and standard deviation (σ) are provided. The calculated temperature (T) ranges (min, max and mean) and ages (cal BCE) are included. Age calibration was achieved using Oxcal 4.4 with the IntCal20 dataset without taking into account a possible hardwater effect. Years marked in red were estimated from the context of the archaeological findings. Modern sites are marked green.

			$\delta^{13}C$ (‰)				$\delta^{18}O$ (‰)				T (°C)			age	
sample	sp.	sec	min	Ø	σ	max	min	Ø	σ	max	min	Ø	max	cal BCE 2σ	
U3041	*M. tub.*	**BS2**	-15.2	-12.3	1.4	-10.8	-2.8	-2.4	0.2	-2.0	23.0	24.8	26.5	425 (CE)	266(CE)
U3043	*M. tub.*	**BS4**	-11.2	-10.5	0.4	-9.6	-3.7	-3.4	0.2	-3.0	27.2	28.9	30.5	1017 (CE)	895 (CE)
U3063	*M. tub.*	**BS5**	-12.2	-11.1	0.5	-9.6	-3.0	-2.5	0.3	-2.1	23.4	25.3	27.2	recent	
U167	*M. tub.*	**KS1**	-9.1	-8.6	0.3	-8.2	-3.0	-2.7	0.2	-2.2	23.8	26.0	27.4	4,356	4,261
U533	*M. tub.*	KS2	-8.4	-7.8	0.3	-7.1	-3.9	-3.6	0.2	-3.1	27.7	30.0	31.1	7,936	7,602
U898	*M. tub.*	**KS52**	-9.8	-9.1	0.3	-8.7	-4.3	-4.1	0.1	-3.8	30.7	32.2	33.0	3,891	3,655
U956-M	*M. tub.*	**KS54**	-8.6	-8.2	0.2	-7.8	-3.2	-3.0	0.1	-2.6	25.8	27.5	28.2	4,346	4,252
U1473-FS1-M	*M. tub.*	**KS54**	-9.5	-9.1	0.3	-8.6	-3.4	-3.0	0.2	-2.7	25.9	27.5	29.1	3,520	3,372
U2335	*M. tub.*	**KS54**	-10.6	-9.9	0.4	-8.7	-3.4	-3.2	0.1	-2.7	26.0	28.3	29.3	3,711	3,642
U1044	*M. tub.*	**KS55**	-10.3	-9.6	0.3	-8.9	-3.3	-3.1	0.1	-2.5	25.1	27.7	28.7	3,522	3,373
U1048	*M. tub.*	**KS55**	-11.4	-10.3	0.7	-8.8	-4.0	-3.7	0.3	-3.1	27.9	30.4	31.8	3,629	3,379
U1049	*M. tub.*	**KS55**	-11.4	-10.7	0.4	-10.1	-3.6	-3.3	0.1	-3.2	28.2	28.9	29.9	3,710	3,639
U1058	*M. tub.*	**KS55**	-9.4	-8.8	0.3	-8.0	-3.0	-2.8	0.1	-2.5	25.4	26.5	27.5	3,632	3,382
U2339-M	*M. tub.*	**KT11**	-9.6	-8.9	0.5	-8.0	-1.8	-1.4	0.1	-1.2	19.7	20.5	22.3	3,076	2,915
U332	*M. tub.*	**LZ5**	-10.2	-9.8	0.1	-9.5	-2.7	-2.4	0.2	-1.9	22.7	24.7	25.9	243 (CE)	353 (CE)
U1972	*M. tub.*	**MD1**	-14.9	-14.1	0.6	-12.5	-3.5	-2.6	0.3	-2.6	25.5	28.1	29.6	recent	
U2523	*M. tub.*	**MD1**	-16.5	-15.4	0.7	-13.6	-3.6	-3.4	0.1	-2.9	26.9	29.1	30.0	recent	

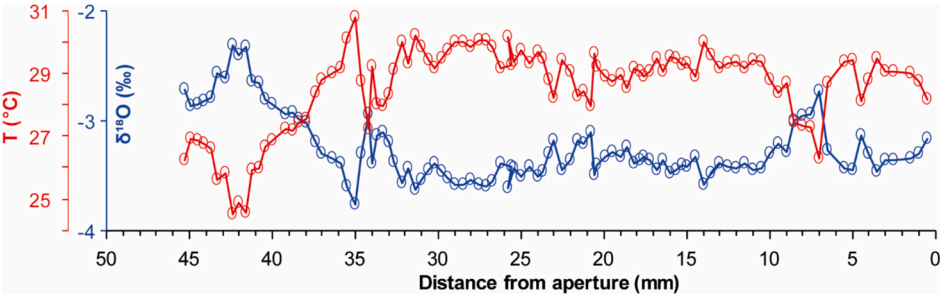

Fig. 6. Stable oxygen isotope data of a *M. tuberculata* snail U2522 (blue) along with reconstructed water temperatures (red). (For interpretation of the references to colour in this figure legend, the reader is referred to the web version of this article.)

3.1.7. Type 2 D: Repeated and continuous slow increase and decrease of $\delta^{18}O_{shell}$ values

Thirty-four *Z. insularis* snails showed a **repeated and continuous, yet slow, $\delta^{18}O_{shell}$ increase followed by slow decrease**. The $\delta^{18}O_{shell}$ signal was more gradual and less distinct than Type 2 C and was repeated between one and three times. The 'cycles' were variable in height and width. (Fig. 11). The snails originated from eighteen sections, including all environmental contexts (Table 8). Carbon isotope values varied between -8.6 ‰ (U2194) and 1.7 ‰ (U1047).

3.1.8. Type 2 E: Rapid change in the $\delta^{18}O_{shell}$ values

Type 2 E showed a **rapid change of up to 1 ‰ between two adjacent $\delta^{18}O_{shell}$ values** (Fig. 12). However, this pattern only occurred in two series of measurements (Table 9), with samples coming specifically from Early Bronze Age contexts (ditch: KS53 and surrounding of Building VII: KS54; Fig. 2). Carbon isotope values varied between -7.0 ‰ (U956-Z) and 0.3 ‰ (U921).

3.1.9. No Signal

The other 44 snails from 14 sections (Table 10) were too brittle for high-resolution analysis. Consequently, due to the limited number of intra-annual samples (2–8 per shell), it was not possible to categorise these snails into the here established Types 2 A–E.

3.2. Isotope signal $\delta^{18}O_{water}$

During fieldwork campaigns in 2022 and 2023, water samples were collected from a single well (Fig. 2), which was continuously fed with groundwater and thus had a constant isotope ($\delta^{18}O_{water}$ = -1.17 ± 0.09 ‰; Fig. 13, red) and temperature (35.72 °C) value. This value was lower than the $\delta^{18}O_{water}$ values calculated from the $\delta^{18}O_{shell}$ reference material from snails living in karst spring water (MD1: 0.46 ± 0.24 ‰; Fig. 13, light green), in the Al-Khashbah *falaj* (KS25: 0.77 ± 0.28 ‰; Fig. 13, green) or in the old oasis of Bisya (BS5: 1.46 ± 0.38 ‰; Fig. 13, dark green).

With one exception (KS52: U898), all shells assigned to Type 1 A (dark blue) were plotted within the range of the Al-Khashbah *falaj* (green) and the karst spring water (light green), as they exhibited a similar range. With three exceptions (SM1: U2526; KT39: U2278; KS6: U4) all shells classified in the Type 1 B (light blue) lie within the range of the signal of the recently abandoned garden (dark green). Of the shells categorised as Type 1 C, eleven out of sixteen are outside the groundwater signal range, and the other five have their average value within, but the high variability within a shell means that their minimum and maximum values are outside.

4. Discussion

The isotopic records presented in this study have been interpreted as changes in the $\delta^{18}O$ of meteoric water, in accordance with the findings of

Table 3
Summary of snails with a $\delta^{18}O_{shell}$ variability between 1 and 2 ‰. The species (sp.: *M. tub.* = *Melanoides tuberculata*), sample name, -section (sec), measured $\delta^{13}C_{shell}$ and $\delta^{18}O_{shell}$ range (min and max) and calculated mean (Ø) and standard deviation (σ) are provided. The calculated temperature (T) ranges (min, max and mean) and ages (cal BCE) are included. Age calibration was achieved using Oxcal 4.4 with the IntCal20 dataset without accounting for a possible hardwater effect. Ages marked in red were estimated from the context of the archaeological findings. Modern sites are marked green.

			$\delta^{13}C$ (‰)				$\delta^{18}O$ (‰)				T (°C)			age	
sample	sp.	sec	min	Ø	σ	max	min	Ø	σ	max	min	Ø	max	cal BCE 2σ	
U2525	*M. tub.*	**BS1**	-7.5	-6.5	0.4	-5.4	-5.0	-4.2	0.4	-3.1	27.9	32.6	36.3	5,210	4,990
U2526	*M. tub.*	**BS1**	-8.2	-7.4	0.3	-6.0	-4.8	-4.1	0.4	-2.9	27.2	31.9	35.0	5,209	4,998
U3061	*M. tub.*	**BS4**	-13.2	-12.2	0.9	-9.9	-3.6	-3.1	0.3	-2.2	23.8	27.7	29.9	822 (CE)	680 (CE)
U3062	*M. tub.*	**BS4**	-12.6	-11.0	1.1	-8.0	-3.9	-3.1	0.3	-2.6	25.5	27.8	31.4	775 (CE)	665 (CE)
U3044	*M. tub.*	**BS5**	-11.9	-10.9	0.8	-8.9	-2.9	-2.1	0.3	-1.4	20.2	23.3	26.7	recent	
U3054	*M. tub.*	**BT1**	-8.1	-7.0	1.1	-3.8	-2.1	-1.7	0.3	-0.8	18.0	21.6	23.5	2,200	2,000
U4	*M. tub.*	**KS6**	-10.4	-9.4	0.6	-8.3	-2.3	-1.5	0.4	-0.8	18.0	21.0	24.4	4,988	4,802
U7	*M. tub.*	**KS6**	-9.8	-8.4	1.1	-4.1	-3.2	-2.4	0.4	-1.5	20.8	24.9	28.2	8,342	8,245
U3069	*M. tub.*	**KS25**	-10.1	-9.4	0.5	-8.1	-3.6	-3.1	0.3	-2.5	25.2	27.7	30.0	recent	
U3070	*M. tub.*	**KS25**	-9.6	-9.1	0.3	-8.4	-3.3	-2.9	0.2	-2.3	24.2	26.9	28.8	recent	
U3117	*M. tub.*	**KS25**	-10.7	-10.1	0.4	-9.1	-3.4	-2.9	0.3	-2.1	23.4	27.1	29.1	recent	
U749	*M. tub.*	**KS32**	-7.7	-6.4	1.1	-3.9	-1.6	-1.2	0.3	-0.5	16.3	19.8	21.4	3,368	3,108
U1043-M	*M. tub.*	**KS54**	-10.2	-9.3	0.5	-7.6	-3.4	-3.0	0.3	-2.3	24.5	27.2	29.3	3,937	3,708
U2331-M	*M. tub.*	**KS54**	-8.8	-7.8	0.4	-7.0	-2.6	-2.0	0.2	-1.5	21.0	22.9	25.6	4,334	4,172
U2337-M	*M. tub.*	**KS54**	-10.2	-9.5	0.4	-7.9	-2.9	-2.5	0.2	-1.9	22.6	25.4	27.0	3,630	3,382
U2203-M	*M. tub.*	**KS54**	-10.5	-9.4	0.5	-7.5	-2.9	-2.4	0.2	-1.8	22.2	24.9	27.0	3,092	2,921
U1064	*M. tub.*	**KS55**	-10.8	-8.7	1.4	-6.8	-3.3	-2.5	0.6	-1.3	20.1	25.1	28.7	3,345	3,100
U1461-M	*M. tub.*	**KS55**	-9.6	-9.2	0.2	-8.5	-2.9	-2.3	0.3	-1.8	22.2	24.5	27.0	3,512	3,365
U1483 -FS8	*M. tub.*	**KS55**	-10.3	-9.8	0.3	-9.3	-3.3	-2.8	0.5	-1.9	22.4	26.4	28.7	3,638	3,528
U2278	*M. tub.*	**KT39**	-11.9	-10.4	0.6	-8.9	-1.8	-1.4	0.3	-0.7	17.2	20.2	22.2	1,615	1,515
U345	*M. tub.*	**LZ5**	-11.9	-10.4	0.5	-9.6	-3.0	-2.6	0.3	-1.8	21.9	25.6	27.2	225 (CE)	328 (CE)
U2522	*M. tub.*	**MD1**	-17.2	-15.3	0.8	-13.1	-3.8	-3.3	0.3	-2.3	24.4	28.5	30.7	recent	
U3051	*M. tub.*	**SM1**	-6.2	-5.5	0.4	-3.8	-7.1	-6.2	0.5	-5.5	38.1	41.1	45.3	6,221	6,069

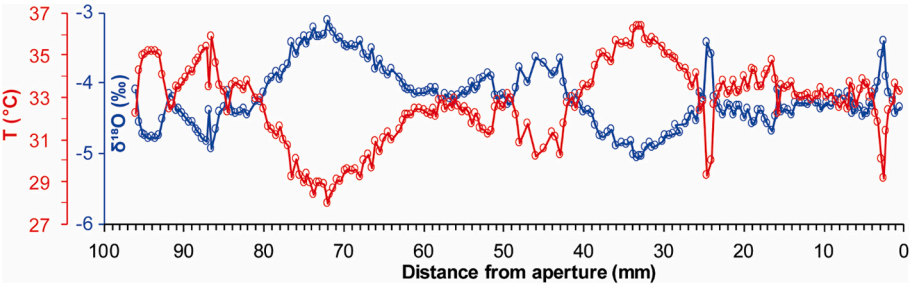

Fig. 7. Stable oxygen isotope data of a *M. tuberculata* snail U2525 (blue) along with reconstructed water temperatures (red). (For interpretation of the references to colour in this figure legend, the reader is referred to the web version of this article.)

Table 4
Summary of snails with a $\delta^{18}O_{shell}$ variability >2 ‰. The species (sp.: *M. tub.* = *Melanoides tuberculata*), sample name, section (sec), measured $\delta^{13}C_{shell}$ and $\delta^{18}O_{shell}$ range (min and max) and calculated mean (Ø) and standard deviation (σ) are provided. The calculated temperature (T) ranges (min, max and mean) and ages (cal BCE) are included. Age calibration was achieved using Oxcal 4.4 with the IntCal20 dataset without accounting for a possible hardwater effect. Years marked in red were estimated from the context of the archaeological findings.

			$\delta^{13}C$ (‰)				$\delta^{18}O$ (‰)				T (°C)			age	
sample	sp.	sec	min	Ø	σ	max	min	Ø	σ	max	min	Ø	max	cal BCE 2σ	
U2524	*M. tub.*	**BS1**	-7.6	-6.4	0.6	-4.7	-5.4	-4.0	0.5	-2.8	26.6	31.8	37.8	5,471	5,309
U2532	*M. tub.*	**KH13**	-9.4	-7.6	1.0	-5.2	-3.0	-1.8	0.6	0.7	11.4	22.1	27.4	5,778	5,659
U23	*M. tub.*	**KS4**	-9.4	-8.1	1.0	-6.2	-4.5	-3.5	0.5	-2.4	24.7	29.7	34.0	7,128	6,828
U8	*M. tub.*	**KS6**	-10.1	-7.9	1.3	-3.9	-3.6	-2.8	0.4	-1.5	21.1	26.3	30.1	5,837	5,716
U13	*M. tub.*	**KS6**	-10.4	-9.0	1.7	-1.4	-3.0	-2.2	1.0	2.2	4.7	23.7	27.3	5,006	4,845
U1451	*M. tub.*	**KS30**	-8.6	-6.8	1.4	-2.9	-2.6	-1.8	0.5	-0.3	15.7	22.2	25.7	3,981	3,805
U1473 -FS2-M	*M. tub.*	**KS54**	-8.8	-8.1	0.4	-6.9	-6.3	-2.6	0.8	-1.6	21.1	25.8	41.8	3,633	3,525
U1067	*M. tub.*	**KS55**	-9.0	-7.9	0.6	-6.8	-1.0	-0.2	0.6	1.2	8.9	15.0	18.8	2,871	2,625
U3076	*M. tub.*	**RW1**	-6.9	-5.9	1.1	-2.2	-6.6	-0.6	1.3	0.0	14.2	16.8	43.0	3,980	3,804
U3077	*M. tub.*	**RW1**	-5.3	-4.3	0.8	-2.3	-7.2	-4.5	2.1	-0.3	15.8	33.9	45.7	3,776	3,653
U3078	*M. tub.*	**RW1**	-7.1	-4.6	1.0	-2.9	-7.2	-4.0	2.3	0.0	14.5	31.9	45.7	3,906	3,656
U3046	*M. tub.*	**SM1**	-7.9	-7.1	0.5	-5.5	-9.5	-8.1	0.6	-7.0	44.7	49.5	55.4	7,138	7,043
U3047	*M. tub.*	**SM1**	-7.7	-6.4	0.6	-5.0	-9.7	-7.8	1.1	-4.9	35.7	48.2	56.6	7,578	7,484
U3048	*M. tub.*	**SM1**	-8.1	-6.7	0.8	-5.2	-9.8	-8.4	0.6	-7.3	45.8	50.7	57.0	7,578	7,484
U3049	*M. tub.*	**SM1**	-8.0	-7.0	0.7	-5.6	-9.5	-8.0	0.6	-7.2	45.5	49.1	55.6	7,534	7,371
U3050	*M. tub.*	**SM1**	-8.2	-7.5	0.4	-5.9	-8.9	-7.9	0.5	-6.8	43.8	48.8	52.9	7,584	7,514

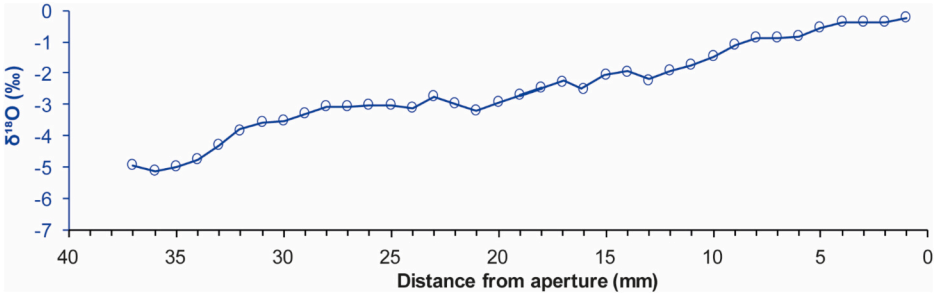

Fig. 8. Stable oxygen isotope data of a *Z. insularis* snail U2277 (blue). (For interpretation of the references to colour in this figure legend, the reader is referred to the web version of this article.)

Table 5
Summary of snails with steadily increasing $\delta^{18}O_{shell}$ values. The species (sp.: *Z. ins.* = *Zootecus insularis*), sample name, section (*sec*), measured $\delta^{13}C_{shell}$ and $\delta^{18}O_{shell}$ range (min and max) and calculated mean (Ø) and standard deviation (σ) are provided. Age calibration was achieved using Oxcal 4.4 with the IntCal20 dataset without accounting for a possible hardwater effect. Years marked in red were estimated from the context of the archaeological findings.

			$\delta^{13}C$ (‰)				$\delta^{18}O$ (‰)				age	
sample	sp.	sec	min	Ø	σ	max	min	Ø	σ	max	cal BCE 2σ	
U3053	*Z. ins.*	**BT1**	-2.2	-1.3	0.5	0.1	1.5	4.9	1.7	7.8	2,200	2,000
U3055	*Z. ins.*	**BT1**	-5.5	-4.6	0.3	-4.3	2.9	5.0	1.3	7.3	2,200	2,000
U3057	*Z. ins.*	**BT1**	-5.4	-4.6	0.5	-3.8	0.9	1.5	0.6	2.7	2,400	2,200
U3075	*Z. ins.*	**BT2**	-6.4	-6.1	0.2	-5.7	0.4	1.7	0.9	3.6	2,400	2,000
U17	*Z. ins.*	**KS4**	-2.2	-1.3	0.3	-0.7	-5.2	-2.5	1.3	-0.3	7,466	7,331
U750	*Z. ins.*	**KS32**	-5.6	-4.2	0.7	-2.5	-5.0	-0.1	2.2	3.1	5,201	4,935
U801	*Z. ins.*	**KS34**	-2.2	-1.5	0.3	-1.0	-1.6	-0.6	0.6	0.5	5,291	5,054
U2204	*Z. ins.*	**KT11**	-11.1	-9.7	0.8	-8.4	1.3	3.5	1.1	5.4	3,339	3,095
U2277	*Z. ins.*	**KT45**	-5.1	-4.2	0.5	-3.0	-6.4	-1.3	2.4	5.0	5,720	5,631

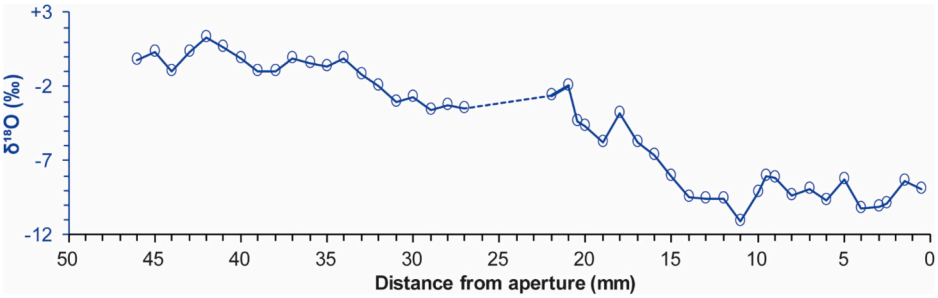

Fig. 9. Stable oxygen isotope data of a *Z. insularis* snail U2337-Z (blue). (For interpretation of the references to colour in this figure legend, the reader is referred to the web version of this article.)

Table 6
Summary of snails showing steadily decreasing $\delta^{18}O_{shell}$ values. The species (sp.: *Z. ins.* = *Zootecus insularis*), sample name, section (sec), measured $\delta^{13}C_{shell}$ and $\delta^{18}O_{shell}$ range (min and max) and calculated mean (Ø) and standard deviation (σ) are provided. The calculated temperature (T) ranges (min, max and mean) and ages (cal BCE) are included. Age calibration was achieved using Oxcal 4.4 with the IntCal20 dataset without accounting for a possible hardwater effect. Years marked in red were estimated from the context of the archaeological findings.

			$\delta^{13}C$ (‰)				$\delta^{18}O$ (‰)				age	
sample	sp.	sec	min	Ø	σ	max	min	Ø	σ	max	cal BCE 2σ	
U2527	*Z. ins.*	**BS1**	-2.2	0.1	1.0	1.7	-6.2	-1.9	2.1	3.3	8,225	7,848
U3052	*Z. ins.*	**BT1**	-6.0	-4.0	1.3	-1.7	-3.1	-0.8	1.4	1.0	2,400	2,000
U918	*Z. ins.*	**KS53**	-5.9	-4.7	0.5	-3.7	-4.8	-0.6	2.6	4.8	5,480	5,376
U919	*Z. ins.*	**KS53**	0.4	1.1	0.4	1.7	-3.9	-0.2	2.3	3.3	8,211	7,857
U1473 -FS2-Z	*Z. ins.*	**KS54**	-10.0	-9.2	0.4	-8.2	2.0	3.7	0.5	4.7	3,487	3,125
U2337-Z	*Z. ins.*	**KS54**	-6.5	-4.3	1.1	-2.6	-11.1	-4.8	3.9	1.3	5,983	5,841

several previous studies of freshwater molluscs (e.g., Dettman et al., 1999; Gajurel et al., 2006; Schöne et al., 2020). It has been demonstrated that shells can record changes in temperature, salinity, flow velocity, river water sources (Versteegh et al., 2011), meteoric water, precipitation (e.g., Dansgaard, 1964; Rozanski et al., 1993), evaporation, (storm) events, catchment (sizes) (Klaus and McDonnell, 2013), and monsoon rainfall (Davis and Muehlenbachs, 2001) as the $\delta^{18}O$ values of the shell reflect the properties of the water in which the

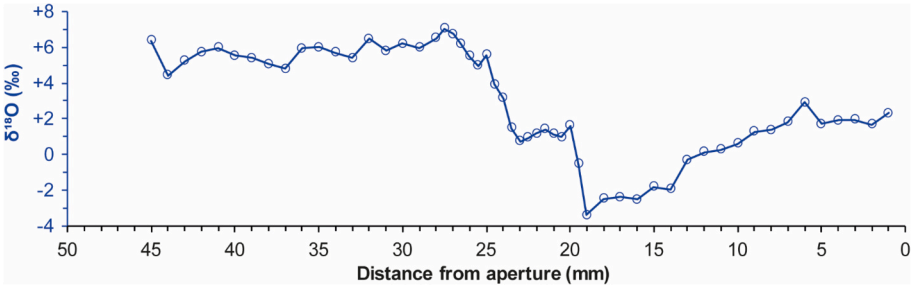

Fig. 10. Stable oxygen isotope data of a *Z. insularis* snail U503 (blue). (For interpretation of the references to colour in this figure legend, the reader is referred to the web version of this article.)

Table 7
Summary of snails showing a sharp and sudden drop in the $\delta^{18}O_{shell}$ values. The species (sp.: *Z. ins.* = *Zootecus insularis*), sample name, section (sec), measured $\delta^{13}C_{shell}$ and $\delta^{18}O_{shell}$ range (min and max) and calculated mean (Ø) and standard deviation (σ) are provided. The calculated temperature (T) ranges (min, max and mean) and ages (cal BCE) are included. Age calibration was achieved using Oxcal 4.4 with the IntCal20 dataset without accounting for a possible hardwater effect. Years marked in red were estimated from the context of the archaeological findings.

			$\delta^{13}C$ (‰)				$\delta^{18}O$ (‰)				age	
sample	sp.	sec	min	Ø	σ	max	min	Ø	σ	max	cal BCE 2σ	
U3060	*Z. ins.*	**BS3**	-5.0	-3.8	0.7	-2.2	-0.1	4.0	2.9	9.0	4,796	4,693
U3072	*Z. ins.*	**BT2**	-4.6	-3.3	0.8	-1.4	4.0	8.8	1.7	11.5	600 (CE)	545 (CE)
U161	*Z. ins.*	**KS1**	-7.5	-6.0	0.8	-3.8	-4.4	-1.5	1.9	1.4	6,750	6,600
U84	*Z. ins.*	**KS2**	0.5	1.0	0.2	1.6	-0.9	1.4	1.4	3.7	8,732	8,560
U38	*Z. ins.*	**KS5**	-0.6	0.5	0.4	1.3	-5.1	-2.3	1.3	0.1	7,040	6,701
U74	*Z. ins.*	**KS5**	-6.6	-4.4	0.9	-2.7	-3.0	-0.7	1.5	2.7	8,288	8,218
U503	*Z. ins.*	**KS6**	-10.9	-9.2	0.7	-7.9	-3.4	2.9	2.9	7.0	605 (CE)	659 (CE)
U566	*Z. ins.*	**KS8**	-2.9	-0.8	0.8	0.3	2.9	6.6	1.7	9.2	4,328	4,063
U728	*Z. ins.*	**KS30**	-5.6	-4.2	0.7	-2.9	0.0	2.7	1.8	5.8	3,651	3,533
U729	*Z. ins.*	**KS30**	-5.5	-4.5	0.8	-3.1	-5.2	-0.5	1.7	2.1	4,446	4,352
U1456	*Z. ins.*	**KS34**	-6.1	-5.4	0.5	-4.2	2.0	4.4	0.8	5.6	5,475	5,332
U1457	*Z. ins.*	**KS34**	-1.0	0.4	0.5	1.4	-1.0	3.7	2.7	7.1	5,980	5,796
U1458	*Z. ins.*	**KS38**	-5.2	-3.8	0.9	-1.0	-1.5	0.5	1.7	4.1	7,311	7,057
U896	*Z. ins.*	**KS52**	-6.9	-4.6	1.2	-1.5	-5.3	-0.9	2.1	2.5	8,536	8,298
U903	*Z. ins.*	**KS52**	-5.7	-5.1	0.4	-4.4	-1.3	2.4	1.8	5.3	6,641	6,481
U1069	*Z. ins.*	**KS55**	-8.4	-6.9	0.7	-5.3	2.5	4.4	0.9	6.4	4,221	3,977
U1482-Z	*Z. ins.*	**KS55**	-9.1	-8.0	0.6	-7.0	1.2	4.8	1.3	6.7	4,445	4,343
U1955	*Z. ins.*	**KS76**	-2.2	-0.3	0.9	1.5	-5.1	-0.9	2.2	4.0	6,461	6,397

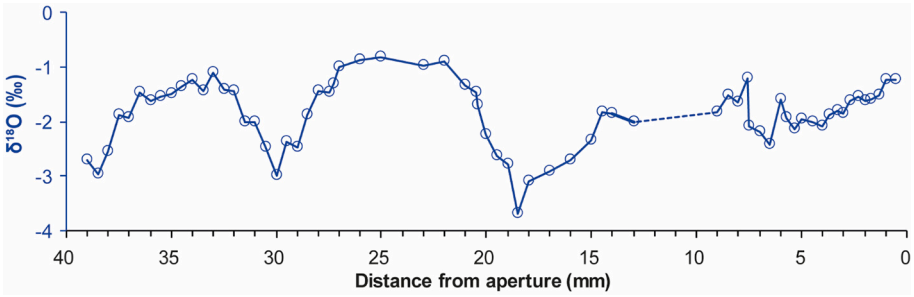

Fig. 11. Stable oxygen isotope data of a *Z. insularis* snail U29 (blue). (For interpretation of the references to colour in this figure legend, the reader is referred to the web version of this article.)

gastropod lived. This principle applies to the aquatic snail *M. tuberculata*, which secretes its shell close to thermodynamic equilibrium with the surrounding water. In contrast, the regulatory mechanisms controlling biomineralization in the terrestrial snail *Z. insularis* are not well understood and can be caused by several environmental factors (see 4.1.2). It is currently unknown whether the shell secretion of *Z. insularis* is in equilibrium with precipitation, dew, and/or humidity. Additionally, it remains unclear whether the rate of shell growth changes under favourable environmental conditions or how fast shell growth is initiated when such conditions emerge.

In general, changes in the isotope variability of meteoric water are based on (1) seasonal variation, (2) variation along altitudinal and latitudinal gradients, (3) variation in the amount of precipitation and (4) the degree of evaporation (Dansgaard, 1964), the latter being a dominant factor in arid areas. Furthermore, it is important to consider (5) reservoir effects, whereby water bodies such as lakes and rivers may have higher $\delta^{18}O$ values due to the evaporation of the lighter isotope. In addition, rivers flowing through specific areas may also have $\delta^{18}O$ values that deviate from local precipitation values, reflective of the origin of their various water inputs (Sjögren and Price, 2013). Moreover,

Table 8
Summary of snails showing a repeated and continuous slow increase followed by slow decrease in the $\delta^{18}O_{shell}$ values. The species (sp.: *Z. ins.* = *Zootecus insularis*), sample name, section (sec), measured $\delta^{13}C_{shell}$ and $\delta^{18}O_{shell}$ range (min and max) and calculated mean (Ø) and standard deviation (σ) are provided. The calculated temperature (T) ranges (min, max and mean) and ages (cal BCE) are included. Age calibration was achieved using Oxcal 4.4 with the IntCal20 dataset without accounting for a possible hardwater effect. Years marked in red were estimated from the context of the archaeological findings.

			$\delta^{13}C$ (‰)				$\delta^{18}O$ (‰)				age	
sample	sp.	sec	min	Ø	σ	max	min	Ø	σ	max	cal BCE 2σ	
U3040	*Z. ins.*	**BT1**	-4.3	-3.6	0.3	-3.0	4.2	5.3	0.7	6.7	2,400	2,000
U3059	*Z. ins.*	**BT1**	-0.5	0.3	0.4	1.3	-0.3	1.8	1.3	4.7	2,400	2,200
U3071	*Z. ins.*	**BT2**	-2.6	-0.8	0.7	0.4	-4.3	0.5	2.8	5.3	198	52
U3073	*Z. ins.*	**BT2**	-2.4	-2.0	0.3	-1.2	-4.9	-4.0	0.7	-2.9	9,308	9,248
U3074	*Z. ins.*	**BT2**	-1.8	-1.4	0.3	-0.9	3.1	4.5	0.8	5.7	1,517	1,439
U2530	*Z. ins.*	**KH13**	-7.5	-5.7	1.2	-2.3	-3.4	0.8	2.2	5.0	7,026	6,650
U2531	*Z. ins.*	**KH13**	-4.3	-2.9	0.7	-1.7	-2.8	0.7	1.3	3.0	6,437	6,261
U158	*Z. ins.*	**KS1**	-4.6	-4.0	0.4	-3.3	-1.9	-0.1	1.0	1.2	6,372	6,097
U532	*Z. ins.*	**KS2**	-4.0	-2.3	1.0	-0.7	-3.3	-0.2	1.3	2.8	7,572	7,372
U28	*Z. ins.*	**KS3**	-2.1	-1.1	0.4	0.0	-2.9	1.3	1.1	2.8	8,279	7,967
U29	*Z. ins.*	**KS3**	-1.2	-0.3	0.5	0.8	-3.7	-1.9	0.6	-0.8	9,801	9,407
U30	*Z. ins.*	**KS3**	-2.6	-2.3	0.2	-2.1	-3.5	-2.7	0.6	-1.8	8,206	7,820
U35	*Z. ins.*	**KS4**	-3.9	-2.3	0.9	-0.5	-2.2	-1.0	0.7	0.6	7,642	7,537
U36	*Z. ins.*	**KS4**	-6.4	-5.6	0.7	-3.7	1.2	1.7	0.4	2.4	6,376	6,101
U37	*Z. ins.*	**KS4**	-2.5	-1.1	0.6	-0.4	-2.4	1.3	1.3	3.3	5,982	5,803
U39	*Z. ins.*	**KS5**	-2.6	-1.6	0.5	-0.4	-1.3	-0.1	0.9	2.2	7,711	7,579
U40	*Z. ins.*	**KS5**	-3.9	-3.2	0.4	-2.1	1.8	2.5	0.4	3.4	4,236	4,046
U80	*Z. ins.*	**KS5**	-4.3	-2.7	1.3	-0.5	-4.5	-1.0	2.0	2.1	6,221	6,067
U501	*Z. ins.*	**KS7**	-5.4	-3.9	0.5	-3.0	4.5	6.3	0.9	8.2	516	398
U569	*Z. ins.*	**KS8**	-7.9	-6.8	0.5	-5.9	-0.6	3.5	2.5	8.2	3,017	2,908
U1453	*Z. ins.*	**KS30**	-2.8	-1.8	0.5	-1.1	-2.3	-0.6	1.1	1.0	6,375	6,090
U834	*Z. ins.*	**KS38**	-0.1	1.0	0.5	1.6	-5.2	-2.6	1.9	1.1	6,464	6,401
U1459	*Z. ins.*	**KS38**	-2.7	-1.9	0.4	-1.3	-6.5	-5.0	0.7	-3.6	11,650	11,529
U1043-Z	*Z. ins.*	**KS54**	-6.5	-5.3	0.7	-3.9	1.4	3.4	1.1	5.9	1,437	1,304
U2203-Z	*Z. ins.*	**KS54**	-6.9	-4.6	1.3	-2.0	-4.7	0.8	2.2	4.6	5,026	4,847
U2331-Z	*Z. ins.*	**KS54**	-6.8	-5.9	0.6	-5.1	5.4	6.4	0.5	7.1	1,509	1,440
U1047	*Z. ins.*	**KS55**	-1.0	0.7	0.4	1.7	-2.0	2.0	2.4	6.9	5,735	5,641
U1466-Z	*Z. ins.*	**KS55**	-7.5	-4.2	1.3	-2.3	0.8	1.9	0.4	2.6	3,641	3,528
U1165	*Z. ins.*	**KS59**	-6.0	-3.5	0.3	1.1	0.5	2.5	1.2	5.0	4,045	3,956
U2194	*Z. ins.*	**KT10**	-8.6	-7.8	0.5	-6.6	-0.4	1.3	0.6	2.5	2,577	2,473
U2199	*Z. ins.*	**KT10**	-6.2	-2.0	1.3	-0.1	-6.0	-3.5	1.4	-0.1	8,215	7,956
U2207	*Z. ins.*	**KT11**	-2.2	-0.3	0.6	0.4	0.8	2.5	1.1	4.9	5,623	5,485
U2339-Z	*Z. ins.*	**KT11**	-8.0	-7.5	0.3	-7.2	2.4	3.2	0.4	3.9	3,640	3,528
U3039	*Z. ins.*	**SM1**	-6.9	-6.0	0.7	-4.6	0.4	2.1	1.1	4.3	7,953	7,744

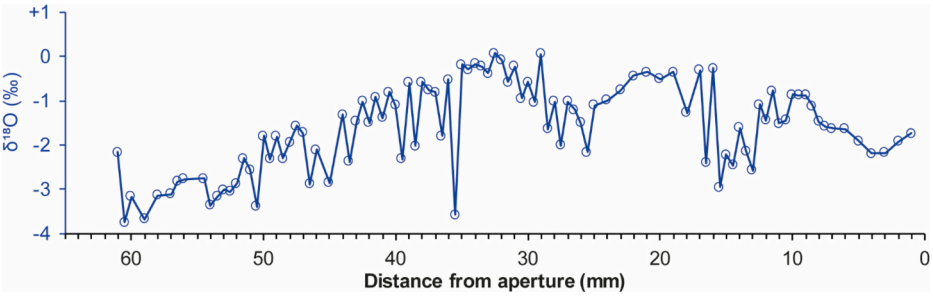

Fig. 12. Stable oxygen isotope data of a *Z. insularis* snail (U921).

Table 9
Summary of snails showing a rapid change of up to 1 ‰ between two adjacent $\delta^{18}O_{shell}$ values. The species (sp.: *Z. ins.* = *Zootecus insularis*), sample name, section (sec), measured $\delta^{13}C_{shell}$ and $\delta^{18}O_{shell}$ range (min and max) and calculated mean (Ø) and standard deviation (σ) are provided. The calculated temperature (T) ranges (min, max and mean) and ages (cal BCE) are included. Age calibration was achieved using Oxcal 4.4 with the IntCal20 dataset without accounting for a possible hardwater effect.

			$\delta^{13}C$ (‰)				$\delta^{18}O$ (‰)				age	
sample	sp.	sec	min	Ø	σ	max	min	Ø	σ	max	cal BCE 2σ	
U921	*Z. ins.*	**KS53**	-3.7	-1.3	1.0	0.3	-3.7	-1.6	1.0	0.1	6,390	6,242
U956-Z	*Z. ins.*	**KS54**	-7.0	-6.1	0.7	-4.3	3.4	5.1	1.1	7.8	3,704	3,632

(6) the continental effect, which results from Rayleigh fractionation, needs to be considered. This effect causes a gradual decrease in isotope ratios during rainout as air masses move inland (Gat et al., 2001). In the Al-Khashbah region, the strength of this effect depends on the trajectories of the air masses, which travel different distances depending on whether they come from the southeast or the north. Furthermore, the Al-

Table 10
Summary of snails originating from a buffered aquatic environment. The species (sp.: *Z. ins.* = *Zootecus insularis*), sample name, section (sec), measured $\delta^{13}C_{shell}$ and $\delta^{18}O_{shell}$ range (min and max) and calculated mean (Ø) and standard deviation (σ) are provided. The calculated temperature (T) ranges (min, max and mean) and ages (cal BCE) are included. Years marked in red were estimated from the context of the archaeological findings. Modern samples are marked green.

			$\delta^{13}C$ (‰)				$\delta^{18}O$ (‰)				age	
sample	sp.	sec	min	Ø	σ	max	min	Ø	σ	max	cal BCE 2σ	
U2528	*Z. ins.*	**BS1**	-3.9	-2.9	0.7	-2.3	0.1	1.8	1.2	2.8	6,453	6,262
U3042	*Z. ins.*	**BS3**	-3.4	-3.3	0.1	-3.2	2.0	2.3	0.3	2.8	4,779	4,558
U3045	*Z. ins.*	**BS6**	-10.1	-9.7	0.3	-9.5	2.8	3.6	0.6	4.2	recent	
U3064	*Z. ins.*	**BS6**	-9.2	-7.9	1.0	-7.1	1.9	2.5	0.5	3.0	recent	
U3065	*Z. ins.*	**BS6**	-11.0	-10.1	0.7	-9.3	3.4	3.9	0.4	4.3	recent	
U3066	*Z. ins.*	**BS6**	-10.5	-10.3	0.2	-10.1	3.5	3.8	0.3	4.1	recent	
U3067	*Z. ins.*	**BS6**	-11.3	-10.9	0.4	-10.5	4.5	5.0	0.6	5.8	recent	
U3068	*Z. ins.*	**BS6**	-7.7	-7.3	0.3	-6.9	3.0	3.1	0.1	3.1	recent	
U3056	*Z. ins.*	**BT1**	0.2	0.4	0.2	0.6	-3.7	-3.1	0.5	-2.2	2,400	2,200
U3058	*Z. ins.*	**BT1**	-0.4	0.2	0.5	0.9	-4.0	-2.7	1.1	-1.4	6,381	6,104
U2533	*Z. ins.*	**KH13**	-7.1	-6.4	0.5	-6.0	-3.1	-2.8	0.2	-2.5	5,725	5,633
U2534	*Z. ins.*	**KH13**	-7.8	-6.6	0.9	-5.6	-2.7	-2.4	0.4	-1.8	5,985	5,837
U2541	*Z. ins.*	**KH13**	-7.8	-7.4	0.3	-7.1	-4.2	-4.1	0.2	-3.9	6,066	5,925
U33	*Z. ins.*	**KS3**	-0.8	-0.6	0.3	-0.5	-0.3	-0.2	0.1	-0.1	7,605	7,538
U576	*Z. ins.*	**KS3**	-0.9	-0.9	0.0	-0.8	-7.0	-5.9	1.0	-4.9	7,952	7,679
U19	*Z. ins.*	**KS4**	-5.2	-4.9	0.2	-4.7	-1.0	-0.9	0.1	-0.8	7,732	7,592
U2186	*Z. ins.*	**KS5**	-0.6	-0.1	0.3	0.1	-5.5	-2.1	2.3	-0.7	7,739	7,596
U2188	*Z. ins.*	**KS5**	-0. 2	0.0	0.2	0.2	-0.9	-0.3	0.4	0.1	9,111	8,635
U2189	*Z. ins.*	**KS5**	-8.0	-7.8	0.1	-7.7	-3.7	-3.1	0.4	-2.7	9,192	8,772
U916	*Z. ins.*	**KS53**	-4.7	-3.8	1.1	-2.6	3.3	4.0	0.7	4.8	7,732	7,596
U2509	*Z. ins.*	**KS54**	-8.7	-8.5	0.3	-8.0	-1.8	-1.7	0.1	-1.6	–	
U2510	*Z. ins.*	**KS54**	-8.5	-8.3	0.1	-8.2	-2.3	-2.3	0.0	-2.2	–	
U2511	*Z. ins.*	**KS54**	-3.2	-2.8	0.3	-2.4	1.1	1.8	1.0	3.2	1,282	1,417
U2512	*Z. ins.*	**KS54**	-0.7	-0.3	0.3	0.1	-0.6	1.4	1.6	3.2	1,496	1,316
U2513	*Z. ins.*	**KS54**	-4.6	-4.0	0.5	-3.6	-0.6	-0.4	0.3	0.1	1,743	1,620
U2514	*Z. ins.*	**KS54**	-9.1	-8.8	0.3	-8.5	-2.2	-2.0	0.2	-1.8	–	
U2515	*Z. ins.*	**KS54**	-8.7	-7.9	0.7	-7.1	-2.6	-2.4	0.1	-2.3	–	
U2516	*Z. ins.*	**KS54**	-10.9	-10.6	0.2	-10.3	-4.2	-4.2	0.1	-4.1	–	
U2517	*Z. ins.*	**KS54**	-4.9	-4.2	0.5	-3.8	2.7	2.8	0.2	3.0	4,445	4,336
U2518	*Z. ins.*	**KS54**	-6.0	-5.6	0.4	-5.1	4.7	7.8	2.1	9.2	2,471	2,302
U2519	*Z. ins.*	**KS54**	-1.3	-0.8	0.5	0.1	3.8	4.4	0.6	5.3	4,443	4,270
U2520	*Z. ins.*	**KS54**	-9.1	-9.0	0.1	-8.9	-3.0	-2.9	0.1	-2.8	–	
U2521	*Z. ins.*	**KS54**	-3.5	-2.5	0.8	-1.8	2.4	4.5	1.6	6.2	3,632	3,381
U1050	*Z. ins.*	**KS55**	-9.2	-7.8	1.2	-5.8	2.2	3.5	0.9	4.8	–	
U1957	*Z. ins.*	**KS76**	-6.4	-6.0	0.5	-5.3	-0.8	-0.4	0.5	0.3	–	
U1961	*Z. ins.*	**KS76**	-3.3	-2.9	0.5	-2.3	0.3	2.4	1.5	3.8	–	
U1963	*Z. ins.*	**KS76**	-0.1	0.3	0.6	1.1	1.2	2.2	1.3	4.0	7,317	7,069
U1966	*Z. ins.*	**KS77**	-6.0	-5.5	0.3	-5.2	-0.9	0.0	0.9	0.9	4,356	4,265
U1967	*Z. ins.*	**KS77**	-2.5	-2.0	0.3	-1.8	0.5	1.6	0.8	2.5	4,994	4,846
U1968	*Z. ins.*	**KS77**	0.1	0.4	0.3	0.8	4.4	4.9	0.4	5.3	5,370	5,221
U1969	*Z. ins.*	**KS77**	-6.0	-5.2	0.5	-4.7	-0.1	0.5	0.5	1.1	4,444	4,336
U1970	*Z. ins.*	**KS77**	-4.9	-4.0	0.8	-2.8	-6.2	-5.7	0.5	-4.9	7,242	7,053
U2338	*Z. ins.*	**KS77**	-17.8	-16.5	1.2	-14.9	-0.9	-0.3	0.6	0.3	-1,024	-900
U2200	*Z. ins.*	**KT10**	-6.2	-6.1	0.1	-6.0	4.4	4.9	0.4	5.2	3,368	3,108

Hajar Mountains can induce an (7) orographic effect. For the sampling localities on the lee side of the mountains, this effect is particularly important. As air masses rise over the mountains, they precipitate most of their moisture on the windward side, where precipitation $\delta^{18}O$ levels are higher, leaving the lee side drier with an ^{18}O-depleted moisture signature. Ultimately, three distinct aquatic systems—atmospheric water (e.g., water vapour from evaporation, rainwater, and atmospheric moisture), surface water (oceans, rivers, streams, and lakes), and groundwater (groundwater, spring systems, and pore water)—are present in Oman either continuously (groundwater and pore water) or occasionally when it rains (streams, pools, and the water vapour produced by their evaporation), making it challenging to interpret the isotope signal recorded by the snails.

4.1. Typology of $\delta^{18}O_{shell}$ values and environmental interpretation

4.1.1. Melanoides tuberculata

The interpretation of palaeoenvironments based on $\delta^{18}O_{shell}$ of freshwater molluscs is a challenging task, as both $\delta^{18}O_{water}$ and temperature can vary significantly depending on the ecohydrological setting. However, the small variation in $\delta^{18}O_{shell}$ values of *M. tuberculata* compared to oxygen isotope data from the terrestrial gastropod *Z. insularis* – which is more directly exposed to $\delta^{18}O_{precipitation}$ signals and likely more significant, air temperature changes – suggests that the studied aquatic specimens inhabit water bodies with varying degrees of environmental buffering (classified as types A–C). This classification can provide insights into the water balance of the respective habitats with distinct hydrological characteristics.

4.1.1.1. Environmental interpretation for Type 1 a: Strongly buffered system. The minor $\delta^{18}O_{shell}$ fluctuations of less than 1 ‰ (Fig. 5) indicate that the snails inhabited buffered water bodies largely unaffected by evaporation, such as groundwater. Oxygen isotopes values in groundwater bodies typically show attenuated $\delta^{18}O_{water}$ variations compared to those of continental water bodies such as lakes, which are especially in these arid conditions prone to evaporation and/or freshwater input like precipitation. However, the narrow range in the specimens of type 1 A suggests an extremely constant $\delta^{18}O_{water}$ signal with only marginal temperature fluctuations. Such conditions are likely due to the predominance of groundwater, as these water bodies lacked external wadi flow supply, rainwater inputs, or evaporative conditions.

This assumption can be strengthened by comparison with modern

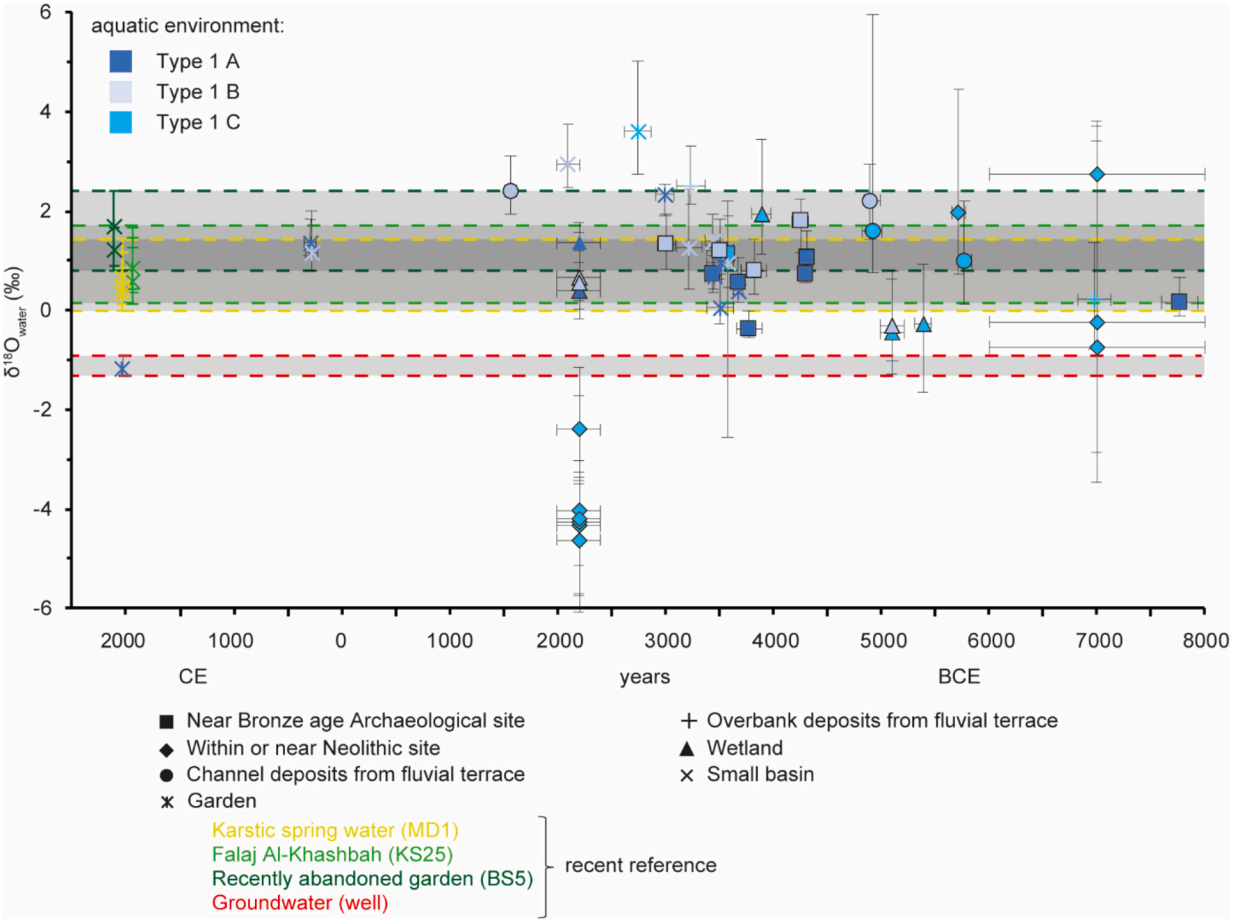

Fig. 13. The calculated $\delta^{18}O_{water}$ values derived from the *M. tuberculata* $\delta^{18}O_{shells}$ data were divided by environmental context (symbols) and colours, according to their $\delta^{18}O_{shells}$ pattern (Type 1 A–C). Error bars indicate the maximum range observed in the data points. The range of the measured $\delta^{18}O_{water}$ values of the Al-Khashbah well is in between the two red dashed lines. The calculated $\delta^{18}O_{water}$ values from the snails from KS25 (*falaj* Al-Khashbah), MD1 (karstic spring water) and BS5 (recently abandoned garden) were represented as green dashed lines, indicating the $\delta^{18}O_{water}$ ranges of different modern water regimes. These values were used as a comparison for the fossil $\delta^{18}O_{water}$ values recorded by the snails. (For interpretation of the references to colour in this figure legend, the reader is referred to the web version of this article.)

representatives of *M. tuberculata* under the current hydrological and temperature conditions. The Al-Khashbah region nowadays has a mean annual air temperature of approximately 28–29 °C (Nizwa, 2019). Average groundwater temperature of the well (35.72 °C), monitored for over a year, exceeded the air temperature. The reconstruction of the water temperatures with $\delta^{18}O_{shell}$ of modern specimens (U332; U1972; U2523, U3063) using the current groundwater oxygen isotope value of -1.17 ‰ yielded an average of 26.2 °C, which is more comparable to the air temperature than to the measured groundwater temperature. Assuming the same groundwater $\delta^{18}O$ value for the fossil specimens, the calculated temperatures of the fossil shells would be slightly higher (maximum 33.0 °C; KS52: U898) than those of modern specimens. However, these temperatures only slightly exceed the typical temperature tolerance of *M. tuberculata*, i.e., 18 to 32 °C (Mitchell and Brandt, 2005). It is possible that the higher temperatures observed in fossil snails result from the use of the modern groundwater oxygen isotope signature, which may have been different in the past due to sea level changes, hydraulic gradients (Weyhenmeyer et al., 2000), different mean residence times of groundwater and groundwater recharge sources (Clark et al., 1987), or variable aquifer reservoirs (e.g., Matter et al., 2006).

With the exception of values reconstructed from U898 (KS52), all $\delta^{18}O_{water}$ data inferred from the studied snails are higher than measured $\delta^{18}O_{water}$ data of groundwater (well), but fall within the observed reference range based on snails from the Al-Khashbah *falaj* (KS25: U3117, U3069, U3070) and specimens from the karstic spring (MD1: U1972; U2522; U2523), both drained with groundwater (Fig. 13). This discrepancy may be attributed to the fact that the water from the well does not reach the surface in the same manner as it does in the karstic spring or the *falaj*, despite the well and the *falaj* originating from the same groundwater system. Furthermore, although we know the depth at which the water snail lives (>20 cm to 2 m; Shanahan et al., 2005), it is impossible to reconstruct the depth of the water and therefore the evaporation rate of the water may be slightly different. Alternatively, the elevated temperatures characteristic of the region may have contributed to the observed increase in the $\delta^{18}O_{water}$ signal, potentially due to evaporation.

4.1.1.2. Environmental interpretation for Type 1 B: Buffered system (with external water inputs?). The variability of $\delta^{18}O_{shell}$ values is higher in Type 1 B snails (Fig. 6) than in Type 1 A, but not as abrupt as expected for a meteorological event such as a cyclone or a storm causing a sudden shift to lower values. The limited range of 1 to 2 ‰ suggests that both periods of water inflow (rain or temporary connection to a wadi flow) and evaporation were sufficiently prolonged to alter the $\delta^{18}O$ value of the water body and ultimately the snail shell. According to the majority of data the isotope changes occurred at a slow and gradual pace. It is proposed that snails of Type 1 B characterise habitats in a buffered system which is not continuously supplied with water or a water body with alternating evaporation and water input phases (like a pool or nowadays *falaj*).

The calculated $\delta^{18}O_{water}$ signal of Type 1 B shells was elevated in comparison to the data measured in the modern well and the signal of Type 1 A shells. However, with the exception of four values (BT1: U3054; KS32: U749; BS4: U3062; BS1: U2526) all the remaining data points fell within the range of the reference snail originating from an irrigated garden (Fig. 13). This discrepancy between the irrigated garden and groundwater signal may be attributed to a greater exposure of the water to evaporation in comparison to Type 1 A. In Oman, these conditions are commonly found in wadis fed by karstic springs (e.g., Wadi Tanuf or Dima Wattayyen), within permanent pools connected to the underflow/inferoflux (e.g., in Wadi Adam, and Wadi Bani Khalid) or within artificial canals draining groundwater to irrigate gardens (*falaj*). However, it is necessary to differentiate between the latter, as there are two types of *aflaj*: The *falaj aini*, which drains spring water, while the *falaj daudi* drains groundwater stored in a shallow aquifer. Both systems transport groundwater through canals to the surface, where it flows overground until it reaches agricultural plots. During the water transport, evaporation may occur, which affects the $\delta^{18}O_{water}$ value and therefore the value.

4.1.1.3. Environmental interpretation for Type 1 C: Open aquatic environment. A $\delta^{18}O_{shell}$ variability larger than 2 ‰ (Fig. 7) suggests that Type 1 C snails experienced significant meteorological events e.g., prolonged droughts leading to increased $\delta^{18}O_{shell}$ values and/or heavy rainfall events resulting in decreased $\delta^{18}O_{shell}$ values. Presumably, Type 1 C shells inhabited an open, highly variable aquatic environment, like those currently prevailing in these wadi systems. Temperature changes occurring during the lifespan of the studied specimens were considerable and reached up to 29 °C. Reconstructed extremes of 62 °C (SM1; U3048) do most certainly not reflect actual water temperature, because studied species could not survive such conditions. They typically occur between 18 and 32 °C (Mitchell and Brandt, 2005). More likely, the isotopic composition of the ambient water body changed as a result of a storm or cyclonic event, resulting in lower $\delta^{18}O_{water}$ values and overestimated temperatures.

The calculated $\delta^{18}O_{water}$ signal was typically lower than the one of modern groundwater (Fig. 13) indicating that these snails recorded either a rainwater signal or the signal of a rainfed hydrosystem characterised by irregular wet and dry phases. In Oman, wadis are dry most of the year, but storm/cyclonic events and flash floods may occur intermittently during the winter rainfall season. These floods can overflow riverbanks or fill small pools, where standing water may persist for days/weeks before it slowly evaporates and infiltrates into the ground.

4.1.2. *Zootecus insularis*

Like aquatic snails, terrestrial gastropods can be used to reconstruct environmental conditions. Following previous studies, the stable oxygen isotope value of terrestrial gastropod shells is mainly influenced by air temperature and humidity as well as the $\delta^{18}O$ signature of water consumed by the snails (e.g., Balakrishnan and Yapp, 2004; Prendergast et al., 2015). The shell oxygen isotope values can be used to determine precipitation, the origin of moisture from which precipitation formed and to infer meteoric water information (Balakrishnan et al., 2005). In this study, the studied terrestrial snails could be assigned to five groups (A, B, C, D and E) based on their $\delta^{18}O_{shell}$ values. Despite the establishment of (regionally) specific equations for the calculation and modelling of palaeotemperatures using various land snail species (e.g., Prendergast et al., 2015; Zanchetta et al., 2005; Balakrishnan and Yapp, 2004), this study initially attempted to employ eq. (1). The temperature ranges obtained fell outside the optimal growth of land snails (7 and 27 °C; Lécuyer et al., 2020), with values ranging from -35.7 °C (BT2; U3072) to 62.6 °C (KS54; U2337-Z). Further research on this topic and on the $\delta^{18}O_{water}$ values computed from the $\delta^{18}O_{shell}$ values of terrestrial snails is required, but is beyond the scope of this study. Additionally, the interpretation of the $\delta^{18}O_{shell}$ signal of the terrestrial snails is a challenging endeavour, as these snails only produce their shell when conditions are optimal (Balakrishnan and Yapp, 2004; Balakrishnan et al., 2005; Lécuyer et al., 2020), which in Oman is limited to a few hours per night due to the arid climate. Furthermore, if conditions are not favourable, these snails enter aestivation, which may account pronounced fluctuations observed in the isotopic datasets.

4.1.2.1. Environmental interpretation for Type 2 A: Strongly evaporative pattern. Gradually increasing $\delta^{18}O_{shell}$ values (Fig. 8) were interpreted as implications for evaporation during periods of high temperature and low humidity. This signal indicates a drying out of or increasingly arid local environment with little or no rainfall to increase the air humidity during the lifetime of the snails. This situation is typical in arid environments such as Oman, which is characterised by high evaporation rates of up to 2200 mm/year and an estimated evaporative rain of 83 % (Abdel-Rahman and Abdel-Magid, 1993). This pattern can be used to identify short-term aridification of an area and/or the presence of a stable arid environment.

4.1.2.2. Environmental interpretation for Type 2 B: continuous freshwater input signal. Specimens documenting a steady $\delta^{18}O_{shell}$ decrease (Fig. 9) were likely exposed to a continuously wetter environment with little or no aridification. This isotope signature does not indicate a rapid or episodic increase in humidity, nor does it show signals of evaporation. It instead represents a stable wet environment, with a tendency for this state to become increasingly pronounced. When those snails are found in deposits showing hydromorphic processes, they seem to match with wetter conditions that prevailed during the Holocene Humid Period and suggest the presence of permanent and stable wetlands. When this signal is found in snails recovered from or near an Early Bronze Age site, it can be interpreted as a striking finding, considering that regional palaeoclimatic data (e.g., Fleitmann et al., 2007; Parker et al., 2016; Beuzen-Waller et al., 2022) indicate the onset of arid conditions by the beginning of the Early Bronze Age (ca. 3,000 BCE). It is therefore proposed that these snails might have recorded the human-induced wet conditions at a local level. In this set, the isotopic data from one snail (U2527) obtained from an overbank deposit near Bisya seems to indicate a palaeo-wetland—apparently active during the Holocene Humid Period according to the age-dating of the snail (8,225–7,848 cal BCE). The other examples (Table 6) came from Early Bronze Age archaeological sites. Specimens U918 and U919 were excavated from the outer ditch of Building XI at Al-Khashbah, U2337-Z and U1473-FS2-Z from the immediate surrounding of Building VII at Al-Khashbah (Fig. 2) and U3052 from an Early Bronze Age building of Rakhat al-Madrh (RAM-3), near Bat. Today, such wet conditions are confined to the immediate vicinity of annual karstic springs, permanent pools surrounded by dense vegetation and anthropogenic environments such as irrigated oases.

4.1.2.3. Environmental interpretation for Type 2 C: Meteorological event signal. In Type 2 C, the sharply dropping $\delta^{18}O_{shell}$ values (Fig. 10) may have recorded a significant and rapid increase in humidity, or this phenomenon may have been triggered by a temporal gap in the documented record, possibly due to aestivation. As this pattern has also been recorded by another terrestrial species from China, where a heavy rainfall event could be precisely linked to the meteorological record of a single super rainstorm event (Wang et al., 2024), the signal is also interpreted here as a heavy rainfall event, such as a summer tropical cyclone or storm (Weyhenmeyer et al., 2000, 2002), which occurs frequently in modern times. In such a case, a significant quantity of ^{16}O is introduced into the system over a relatively short time interval. Following the event, the environment gradually becomes drier because of evaporation. This results in $\delta^{18}O_{shell}$ values returning to their pre-event levels.

4.1.2.4. Environmental interpretation for Type 2 D: Cyclic weather variation signal. Like in the Type 2 C specimens, both evaporation and freshwater influx are visible in the Type 2 D pattern (Fig. 11). However, in these specimens, the $\delta^{18}O_{shell}$ signal is more continuous without sharp drops and is repeated. This pattern may indicate a slow change in environmental conditions, such as a seasonal shift between prolonged wet and dry seasons alternating periodically, with variable width and height in the signal attributed to the fact that the environmental conditions are not consistent from year to year. In the absence of published data on the annual growth rate of this terrestrial snail species, it is not possible to estimate the duration of the aforementioned time intervals, particularly given the absence of visible growth increments. This makes it difficult to compute the duration of the wet and dry phases/season. A consistent rainfall/water input source and stable environmental conditions can be inferred when the isotopic signatures exhibit similar minima and maxima values (Fig. 11).

A comparison of the $\delta^{18}O_{speleothem}$ data reveals discrepancies with the $\delta^{18}O_{shell}$ data. Previous studies have examined speleothem isotopic signatures for rainfall origin (Burns et al., 1998, 2001; Weyhenmeyer et al., 2000, 2002; Fleitmann et al., 2003), by considering the Rayleigh effect, which postulates a gradual depletion of isotope ratios with rainfall (Gat et al., 2001). In the case of Oman, this means that the isotopic signature of rain coming from the north (Eastern Mediterranean; winter depressions), is isotopically enriched, compared to that of rain coming from the south (Indian Ocean; monsoons and cyclones) (Burns et al., 1998, 2001; Weyhenmeyer et al., 2000, 2002; Fleitmann et al., 2003). The speleothems of the Hoti Cave recorded a $\delta^{18}O$ range between -6 and -4 ‰ from 9,500 to 6,300 BCE (Holocene Humid Period), indicative of high monsoonal precipitation inputs. The fourteen snails dated to this period exhibit a considerably wider $\delta^{18}O_{shell}$ span, ranging from -5.0 to 1.7 ‰. In the subsequent period, the values of the speleothems increased to approximately -3‰3 ‰, indicating a reduction in monsoon precipitation, with most precipitation originating from the north (Mediterranean Sea) (Fleitmann & Matter, 2009). The twenty shells that are younger than 6,300 BCE exhibit a considerably broader range, spanning from -4 to 6.4 ‰. Further research is required to elucidate whether the observed discrepancies can be attributed to metabolic effects or differences in the chemical composition of the calcite and aragonite present in the speleothems and snails, respectively. Since both snails and speleothems require different conditions for optimal growth, it is plausible that they have documented distinct conditions.

4.1.2.5. Environmental interpretation for Type 2 E: rapid wet/dry cycle. The rapid isotopic shifts of Type 2 E shells (Fig. 12) may indicate an unstable environment with significant changes in the environmental conditions, either caused by unfavourable environmental conditions, so that the snail enters to aestivation, or by man-made environmental changes. As the first possibility cannot be confirmed, because other environmental records, such as speleothems or pollen, are either not available or do not have such a high resolution for comparison, we suggest the second possibility, because the shifts are very frequent in some cases. The decreasing $\delta^{18}O_{shell}$ values are likely to be caused by repeated freshwater input over short intervals of time while the increasing values may be caused by short-term evaporation without fully drying out. Such conditions can be observed in irrigated gardens that are regularly watered but not flooded continuously. U921 (ditch) and U956-Z were found in the vicinity of Early Bronze Age sites. Since that time, climate presumably was as arid as today (Fleitmann et al., 2007; Parton et al., 2015). It is hypothesized that these snails were either older and relocated, and recorded a climate characterised by repeated short-term water input alternating with evaporation or that they recorded artificial watering in the surroundings of Early Bronze age sites.

4.2. Correlation between context of sampling and isotope signal

To evaluate the correlation between sampling context and the isotopic pattern, the aquatic and the terrestrial snails were evaluated separately. Two signal types (Type 1 A and 2 A) align closely with the environmental context of sampling. The majority of aquatic snails classified as Type 1 A, a “strongly buffered environment”, originate from either a hydromorphic unit or an oasis garden. These two environments are influenced by groundwater, either naturally or artificially. Terrestrial snails classified as Type 2 A (evaporation pattern) were primarily sourced from two environments, namely overbank deposits and depressions (Fig. 3). These environments are rarely flooded and are exposed to prevailing evaporative conditions (Fig. 14). Further research is required to ascertain the duration of the drought by analysing the shell growth parameters.

Type 2 C and D shells were particularly useful indicators of seasonal environmental changes and events because they were found in each studied archaeological context (Fig. 14). More generally, snail shells can serve as a key archive to study palaeo-rainfall in drylands, because they are not limited to specific contexts (Girod and Sassoon, 2022) and can record (even small) rainfall events (Dong et al., 2022; Wang et al., 2024). Furthermore, it is conceivable that snail shells may record repeated rainfall or flooding events (e.g., Fig. 11). This would provide valuable insights into the frequency of rainfall and flooding and their potential origins. It is important to note that the snails only record brief weather and seasonal fluctuations, as they have relatively short lifespans. This limits the ability to speak of climate based on their data. Indeed, further studies are required to ascertain the maximum lifespan of a snail, with previous studies yielding highly variable ranges from 2 to 7 years (Heller, 1990). Finally, the process of shell secretion requires further investigation (see Section 4.3).

This study also documented the evolution of environmental signals observed in aquatic snails sampled from Neolithic and Bronze Age archaeological sites. Isotope signals reflected a diachronic transition from an open environment (surface water) to a buffered environment (groundwater). The majority of the aquatic snails collected from Neolithic sites were indicative of open system environments (Type 1 C), such as wadis, suggesting the presence of rain-fed surface water in the vicinity of the site during its occupation. This is consistent with the current understanding of the prevailing conditions during the Neolithic, which are characterised by a humid climate (Holocene Humid Period) enabling the accessibility of surface water. Conversely, aquatic snails collected from or in the vicinity of Early Bronze Age sites, recorded a buffered to strongly buffered environment, indicating that the sites were in close proximity to a groundwater outcrop or groundwater discharge area, such as those prevailing near *falaj* irrigation system or springs. This information is of interest because the water management during the Early Bronze Age is not well attested in the region (Charbonnier, 2015). Furthermore, the recurrent pattern in Early Bronze age settlement location may also indicate that Early Bronze Age societies chose to settle in areas with a shallow water table or where groundwater was accessible. This strategy can be explained by a decrease of the rainfall, in conjunction with the southward migration of the monsoon (Fleitmann et al., 2007; Parton et al., 2015). However, due to ^{14}C dating uncertainties, it is still impossible to place shells in accurate temporal context.

By including the ^{14}C ages of the studied aquatic snails (without correction of the hardwater effect), the average age obtained for snails coming from Neolithic contexts (6,066–5,633 cal BCE) matched well with the chronology of the Neolithic period (6,000–3,200 BCE). In the Early Bronze Age contexts (3,200–2,000 BCE), the ^{14}C dates exhibited greater variability (ranging from 7,936 to 2,921 cal BCE). This suggests that some of the studied specimens (i.e., the oldest ones) were allochthonous and might be biased by a hardwater effect (Lindauer et al., 2018). Further research is required to ascertain whether the relative age dating provided by the stratigraphic context is more reliable

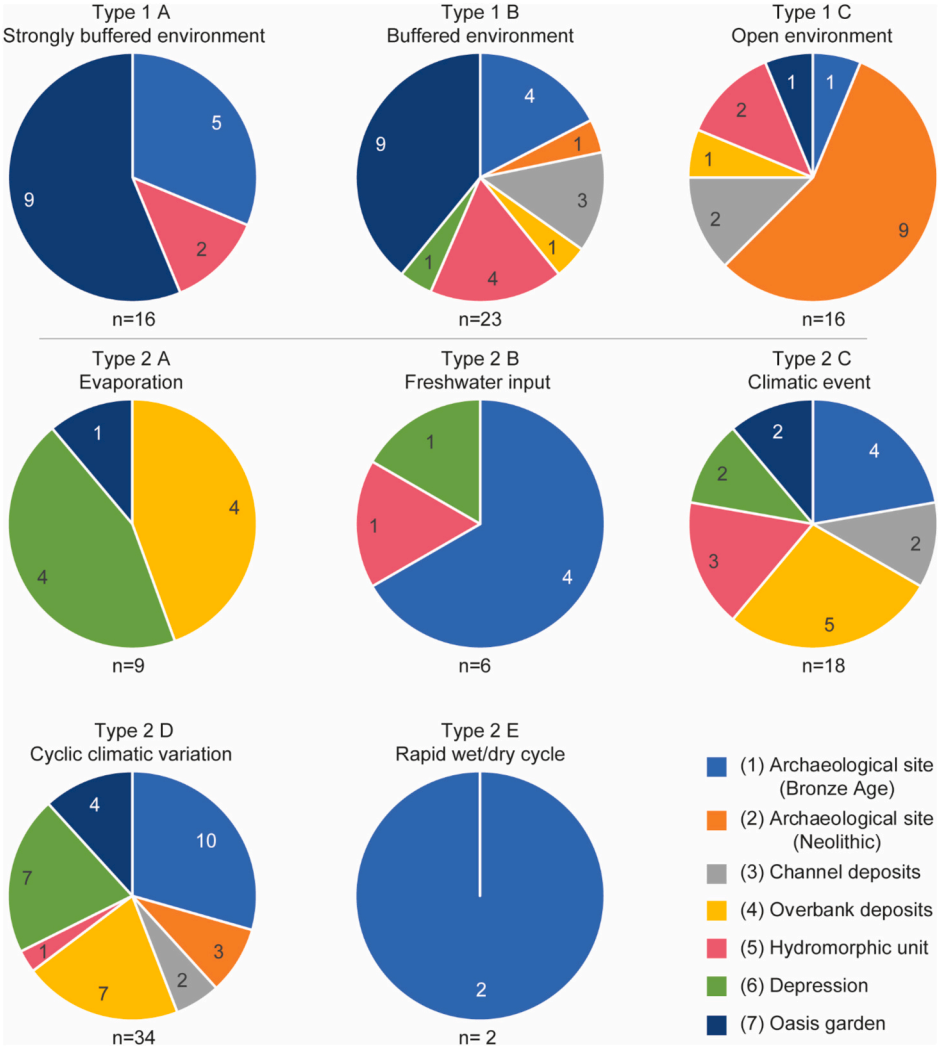

Fig. 14. Pie charts depicting the relative proportion of contexts in which shells with a given signal type were recovered. Type 1 refers to *M. tuberculata* shells while Type 2 refers to *Zootecus insularis*. See Results section for a detailed description.

than the absolute age dating when using snails as a geoarchaeological proxy in arid environments.

4.3. Limits and further investigation

Although there are studies on high-resolution sampling of other terrestrial snail species (e.g., Leng et al., 1998; Long et al., 2020; Dong et al., 2022; Li et al., 2024), this is the first study to sample both terrestrial *Z. insularis* and freshwater/brackish water *M. tuberculata* snails from the same arid environment at unprecedented high resolution and use their isotope data to reconstruct environmental conditions. Although others have interpreted the data with other species here are still some issues that require further investigation: First, diagenetic alteration of aragonite is a persistent concern (Swart, 2015 and references therein). It may be caused by temperature (Ritter et al., 2017; Forjanes et al., 2022), meteoritic water, time (Lindauer et al., 2018; Milano et al., 2018) and anthropogenic burning within archaeological sites. The latter factor is not considered due to the non-consumable nature of the snails and their locations, which are not in the vicinity of fireplaces. Considering the relatively young geological age of the snails (oldest U1459: 11,650 cal BCE) the time factor was as well, leaving temperature and meteoric water as the remaining possibilities for post-depositional isotope changes. The temperature-induced decomposition of the organic matrix of a shell can cause the precipitation of abiogenic aragonite at temperatures between approximately 80 and 175 °C (Forjanes et al., 2022). Although Al-Khashbah does not experience temperatures as high as 80 °C, Swart (2015) suggests that early diagenetic alterations tend to occur at temperatures between 20 °C and 30 °C, which are commonly reached in Oman (highest temperatures recorded by a HOBO data logger placed in a tree 10 cm above the ground near Al-Khashbah: 47.5 °C). Furthermore, the fog caused by temperature fluctuations can act as a fluid required to facilitate abiogenic aragonite precipitation and associated isotopic changes. Finally, in Oman, floods during the rainy season can expose the snails to varying temperatures (daily fluctuations of up to 20 °C) and chemical compositions of fluids.

Another factor to be considered is the post-mortem transportation and/or relocation of snails due to unstable depositional environments (such as flooplain). Especially the terrestrial snails are are often moved by water (rain and rivers) (Girod and Sassoon, 2022 and references therein) before they are finally deposited. It is possible that the snails may be relocated vertically (during the excavation of sediments and/or bioturbation) or horizontally (due to floods, wind or human activity, for example, in mudbricks, which were a common building material used in Early Bronze Age construction). It is likely that the relocation was limited to short distances, because further transport during strong flow of flash floods would have increased the probability of damage. Nevertheless, there were some areas where the snails were relatively

protected, e.g., if they were incorporated into mudbrick materials. This is probably the primary reason for the long-term preservation of Early Bronze Age shells. It needs to be pointed out that the reconstructed environmental conditions pertain to the area where the shells originally lived, rather than the stratigraphic layer where they were discovered. The paucity of existing studies on this topic serves to illustrate a gap in the understanding of these taphonomic processes, underscoring the need for further investigation in order to accurately interpret the environmental histories from shell assemblages.

Radiocarbon dating of terrestrial and freshwater shells poses significant challenges resulting from a possible hardwater effect (Lindauer et al., 2017, 2018; Lindauer, 2019; Philippsen, 2013). ^{14}C dates of shells reflect the age of the carbon in the environment in which the snail lived as well as its food resource. This carbon eventually becomes incorporated into the shell calcium carbonate throughout life. Freshwater snails use dissolved inorganic carbon in the water to build up their shell whereas terrestrial shells digest the carbon from food and soil. Depending on the source, this can lead to a radiocarbon age that is shifted in comparison with the true calendar age of the shell which is described as hardwater effect. In contrast to the marine reservoir effect that usually comprises at most around 1000 years, the hardwater effect can easily account for over 3,000 years (Philippsen and Heinemeier, 2013). It is recommended that the age of a stratigraphic layer is determined by ^{14}C-dating rather than the shell itself. This can be achieved by dating a large set of shells found in a single sedimentary layer and/or a multiproxy dating approach including cross age dating of charcoal, humic acid, etc. and optically stimulated luminescence (OSL).

It is also of great importance to gain an understanding of the rate of shell formation and growth in terrestrial snails under both optimal and suboptimal humidity and temperature conditions. Additionally, further studies are required to correlate live-collected terrestrial snail data with recorded environmental data, which is essential for future research in that region. This represents another area for further research. Furthermore, the indistinct growth lines of both species make it challenging to determine the specific period of growth, a limitation that is also present in the classical sclerochronology of shells (e.g., Schöne and Surge, 2012; Taft et al., 2014). It will also be imperative to determine whether both species possess an inner and outer shell layer, given that the shells are fragile and may be pierced during drilling (Fig. 4). This necessitates an investigation into whether the two layers, if present, exhibit an isotopic offset and if it is necessary to examine them separately, if feasible. However, this is beyond the scope of the present study.

5. Conclusion

In this study, the stable oxygen isotope values of aquatic (*M. tuberculata*) and terrestrial (*Z. insularis*) snail shells were determined. Specimens were recovered from specific archaeological, geomorphological and modern contexts with the goals of investigating their potential as a snapshot insight into past hydroclimatic and palaeoenvironmental conditions in drylands, correlating their environmental context with a specific $\delta^{18}O_{shell}$ pattern. Additionally, the $\delta^{18}O$ signature of the groundwater was determined and temperature data were collected. The comparison between the stable oxygen isotope data of aquatic (*M. tuberculata*) and terrestrial (*Z. insularis*) snails and the areas of sampling enabled the extraction of eight distinct environmental signals, differentiated by aquatic (Type 1) and terrestrial (Type 2) environments in which those types of snails lived. The interpretation of this data represents a preliminary attempt to develop a typology of isotopic signals based on $\delta^{18}O$ variations in snail shells, aiming to elucidate environmental and hydrological conditions. The proposed typology includes: **Type 1 A:** In a strongly buffered aquatic environment, minimal $\delta^{18}O_{shell}$ variations (< 1 ‰) indicate the presence of stable groundwater sources, reflecting a relatively constant isotopic composition. **Type 1 B:** In a buffered aquatic environment, $\delta^{18}O_{shell}$ variations range from 1 to 2 ‰. This suggests occasional inputs from a wadi, rainwater inflow, and subsequent evaporation, indicating moderate variability in water sources and environmental conditions. **Type 1 C:** In an open aquatic environment, large variations (> 2 ‰) in $\delta^{18}O_{shell}$ highlight a highly variable environment. These pronounced shifts may reflect rapid responses to environmental changes, such as prolonged droughts or fluctuations in water supply. **Type 2 A:** Consistently increasing $\delta^{18}O_{shell}$ values hint at exposure to a drying environment, potentially reflecting a trend towards arid conditions or reduced water availability. **Type 2 B:** A continuous decrease in $\delta^{18}O_{shell}$ values denotes steady freshwater input, likely from a stable and continuous source such as a river or precipitation, reflecting a more humid and stable hydrological condition. **Type 2 C:** Sharp drops in $\delta^{18}O_{shell}$ values reveal a meteorological event, such as heavy rainfall associated with cyclones. These sudden changes may be followed by dry periods, suggesting significant weather fluctuations. **Type 2 D:** Repeated and slow increases followed by decreases in $\delta^{18}O_{shell}$ values imply alternating periods of evaporation and freshwater influx. This pattern suggests seasonal shifts between prolonged wet (monsoonal) and dry seasons. **Type 2 E:** Rapid and strong short-term fluctuations in $\delta^{18}O_{shell}$ values reflect high-frequency changes in water input and evaporation, potentially caused by human activities such as irrigation (in a modern context), revealing anthropogenic influences on the environmental system. Surprisingly, most of the aquatic snails in this study lived in groundwater and therefore recorded either a pure groundwater signal (Type 1 A; strong buffered system) or a groundwater-fed environmental signal with slight evaporation and freshwater influxes (Type 1 B; buffered system). Finally, the results obtained from the archaeological sites indicate that aquatic snails may be a reliable indicator of ancient irrigation systems or water management practices exploiting groundwater, which could prove to be a valuable tool for future geoarchaeological research in dryland regions. In conclusion, the findings of this study provide support for further scientific development of sclerochronology with gastropods, which is currently a largely underutilised area of research.

CRediT authorship contribution statement

Katharina E. Schmitt: Visualization, Writing – original draft, Supervision, Project administration, Methodology, Investigation, Funding acquisition, Data curation, Conceptualization. **Tara Beuzen-Waller:** Writing – original draft, Visualization, Project administration, Methodology, Investigation, Funding acquisition, Data curation, Conceptualization. **Conrad Schmidt:** Writing – review & editing. **Lucas Proctor:** Writing – review & editing. **Susanne Lindauer:** Writing – review & editing. **Christoph J. Gey:** Writing – review & editing. **Dana Pietsch:** Writing – review & editing. **Bernd R. Schöne:** Writing – review & editing, Funding acquisition.

Declaration of competing interest

The authors declare the following financial interests/personal relationships which may be considered as potential competing interests:

Katharina E. Schmitt reports financial support was provided by Federal Ministry of Education and Research Bonn Office. If there are other authors, they declare that they have no known competing financial interests or personal relationships that could have appeared to influence the work reported in this paper.

Data availability

we provide the supplements as an Excel file

Acknowledgements

We thank Michael Maus (JGU Mainz) for laboratory assistance and Hubert Vonhof (Max Planck Institute for chemistry, Mainz) for $\delta^{18}O_{water}$ measurements. The high-resolution sampling of the snails is owed to

Anka Carina Meßmer (JGU Mainz) and Leonie Lange (University of Potsdam). Financial support from the German Federal Ministry of Education and Research (BMBF) for the project UmWeltWandel under grant no. 01UL2001A and 01UL2001B is gratefully acknowledged. We thank the archaeological project and collaborators that help us to gather this collection: Vincent Charpentier, Stephanie Döpper, Mathilde Jean, Maria Pia Maiorano, Aleksandre Prosperini, Jennifer Swerida, Martin Sauvage.

Appendix A. Supplementary data

Supplementary data to this article can be found online at https://doi.org/10.1016/j.palaeo.2024.112542.

References

Abdel-Rahman, H.A., Abdel-Magid, I.M., 1993. Water conservation in Oman. Water Intern. J. 18, 95–102. https://doi.org/10.1080/02508069308686155.

Abell, P.I., 1985. Oxygen isotope ratios in modern African gastropod shells: a data base for paleoclimatology. Chem. Geol.: Isotope Geosci. Sect. 58 (1–2), 183–193. https://doi.org/10.1016/0168-9622(85)90037-5.

Al-Khayat, J.A., 2010. First record of five terrestrial snails in the State of Qatar. Turk. J. Zool. 34 (4), 539–545. https://doi.org/10.3906/zoo-0807-26.

Andreou, G.M., Westley, K., Huigens, H.O., Blue, L., 2022. Exploring the impact of tropical cyclones on Oman's maritime cultural heritage through the lens of Al-Baleed, Salalah (Dhofar Governorate). J. Marit. Archaeol. 17 (3), 465–486. https://doi.org/10.1007/s11457-022-09333-4.

Armitage, S.J., Jasim, S.A., Marks, A.E., Parker, A.G., Usik, V.I., Uerpmann, H.-P., 2011. The Southern Route 'out of Africa': evidence for an early expansion of Modern Humans into Arabia. Science 331 (6016), 453–456. https://doi.org/10.1126/science.1199113.

Balakrishnan, M., Yapp, C.J., 2004. Flux balance models for the oxygen and carbon isotope compositions of land snail shells. Geochim. Cosmochim. Acta 68 (9), 2007–2024. https://doi.org/10.1016/j.gca.2003.10.027.

Balakrishnan, M., Yapp, C.J., Theler, J.L., Carter, B.J., Wyckoff, D.G., 2005. Environmental significance of $^{13}C/^{12}C$ and $^{18}O/^{16}O$ ratios of modern land-snail shells from the southern great plains of North America. Quat. Res. 63 (1), 15–30. https://doi.org/10.1016/j.yqres.2004.09.009.

Beuzen-Waller, T., 2020. Interactions entre dynamiques environnementales et occupations humaines du Paléolithique à l'âge du Fer dans les piémonts du Jebel Hajar (Oman). Doctoral dissertation. Sorbonne université.

Beuzen-Waller, T., Desruelles, S., Marrast, A., Giraud, J., Gernez, G., Forman, S., Beshkani, A., Bonilauri, S., Lemée, M., Nacarro, H., Fouache, E., 2022. Late Pleistocene-Holocene fluvial records of the Wadi Dishshah: hydro-climatic and archaeological implications (Southern piedmont of the Hajar Mountains, Oman). Géomorphol. Relief, Proc. Environn. https://doi.org/10.4000/geomorphologie.17247.

Blechschmidt, I., Matter, A., Preusser, F., Rieke-Zapp, D., 2009. Monsoon triggered formation of Quaternary alluvial megafans in the interior of Oman. Geomorphology 110 (3–4), 128–139. https://doi.org/10.1016/j.geomorph.2009.04.002.

Breeze, P.S., Groucutt, H.S., Drake, N.A., White, T.S., Jennings, R.P., Petraglia, M.D., 2016. Palaeohydrological corridors for hominin dispersals in the Middle East~250–70,000 years ago. Quat. Sci. Rev. 144, 155–185. https://doi.org/10.1016/j.quascirev.2016.05.012.

Burns, S.J., Fleitmann, D., Matter, A., Neff, U., Mangini, A., 2001. Speleothem evidence from Oman for continental pluvial events during interglacial periods. Geology 29 (7), 623–626.

Burns, S.J., Matter, A., Frank, N., Mangini, A., 1998. Speleothem-based paleoclimate record from northern Oman. Geology 26 (6), 499–502.

Charbonnier, J., 2015. Groundwater management in Southeast Arabia from the Bronze Age to the Iron Age: a critical reassessment. Water History 7, 39–71. https://doi.org/10.1007/s12685-014-0110-x.

Clark, I.D., Fritz, P., Quinn, O.P., Rippon, P.W., Nash, H., Sayyid, B.B.G.A.S., 1987. Modern and fossil groundwater in an arid environment: a look at the hydrogeology of southern Oman. In: Isotope Techniques in Water Resources Development.

Dansgaard, W., 1964. Stable isotopes in precipitation. T*ellus* 16 (4), 436–468. https://doi.org/10.1111/j.2153-3490.1964.tb00181.x.

Davis, L.G., Muehlenbachs, K., 2001. A late Pleistocene to Holocene record of precipitation reflected in *Margaritifera falcata* shell $\delta^{18}O$ from three archaeological sites in the lower Salmon River Canyon, Idaho. J. Archaeol. Sci. 28 (3), 291–303. https://doi.org/10.1006/jasc.2000.0562.

De Kock, K.N., Wolmarans, C.T., 2009. Distribution and habitats of *Melanoides tuberculata* (Müller, 1774) and *M. victoriae* (Dohrn, 1865)(Mollusca: Prosobranchia: Thiaridae) in South Africa. Water SA 35 (5). https://doi.org/10.4314/wsa.v35i5.49197.

Dettman, D.L., Reische, A.K., Lohmann, K.C., 1999. Controls on the stable isotope composition of seasonal growth bands in aragonitic fresh-water bivalves (Unionidae). Geochim. Cosmochim. Acta 63 (7–8), 1049–1057. https://doi.org/10.1016/s0016-7037(99)00020-4.

Dong, J., Yan, H., Zong, X., Wang, G., Liu, C., Xing, M., Lan, J., Wei, G., Dodson, J., An, Z., 2022. Ultra-high resolution $\delta^{18}O$ of land snail shell: a potential tool to reconstruct frequency and intensity of paleoprecipitation events. Geochim. Cosmochim. Acta 327, 21–33. https://doi.org/10.1016/j.gca.2022.04.015.

Elgamal, M.H., Awadallah, A.G., Badry, H., 2007. Hydrological analysis of Cyclone Gonu. A case study: Wadi al Zyhimi. In: Fourth International Conference on Wadi Hydrology. Sultanate of Oman, Muscat.

Fleitmann, D., Burns, S.J., Neff, U., Mangini, A., Matter, A., 2003. Changing moisture sources over the last 330,000 years in Northern Oman from fluid-inclusion evidence in speleothems. Quat. Res. 60 (2), 223–232. https://doi.org/10.1016/s0033-5894(03)00086-3.

Feulner, G.R., Green, S.A., 2003. Terrestrial molluscs of the United Arab Emirates. *Mitt. dtsch. malakozool.* Ges 69 (70), 23–34.

Fleitmann, D., Burns, S.J., Mangini, A., Mudelsee, M., Kramers, J., Villa, I., Neff, U., AlSubbary, A.A., Buettner, A., Hippler, D., Matter, A., 2007. Holocene ITCZ and Indian monsoon dynamics recorded in stalagmites from Oman and Yemen (Socotra). Quat. Sci. Rev. 26, 170e188. https://doi.org/10.1016/j.quascirev.2006.04.012.

Fleitmann, D., Burns, S.J., Pekala, M., Mangini, A., Al-Subbary, A., Al-Aowah, M., Kramers, J., Matter, A., 2011. Holocene and Pleistocene pluvial periods in Yemen, southern Arabia. Quat. Sci. Rev. 30 (7–8), 783–787. https://doi.org/10.1016/j.quascirev.2011.01.004.

Fleitmann, D., Matter, A., 2009. The speleothem record of climate variability in Southern Arabia. Comptes Rendus. Géosci. 341 (8–9), 633–642.

Fontes, J.C., Gasse, F., Andrews, J.N., 1993. Climatic conditions of Holocene groundwater recharge in the Sahel zone in Africa. In: Isotope Techniques in the Study of Past and Current Environmental Changes in the Hydrosphere and the Atmosphere. https://doi.org/10.1016/s0048-9697(96)05326-0.

Forjanes, P., Simonet Roda, M., Greiner, M., Griesshaber, E., Lagos, N.A., Veintemillas-Verdaguer, S., Astilleros, J.M., Fernández-Díaz, L., Schmahl, W.W., 2022. Experimental burial diagenesis of aragonitic biocarbonates: from organic matter loss to abiogenic calcite formation. Biogeosciences 19 (16), 3791–3823. https://doi.org/10.5194/bg-19-3791-2022.

Gajurel, A.P., France-Lanord, C., Huyghe, P., Guilmette, C., Gurung, D., 2006. C and O isotope compositions of modern fresh-water mollusc shells and river waters from the Himalaya and Ganga plain. Chem. Geol. 233 (1–2), 156–183. https://doi.org/10.1016/j.chemgeo.2006.03.002.

Gat, J.R., Mook, W.G., Meijer, H.A., 2001. Environmental isotopes in the hydrological cycle. *Principles and Applications UNESCO/IAEA*. Series 2, 63–67.

Ghosh, P., Rangarajan, R., Thirumalai, K., Naggs, F., 2017. Extreme monsoon rainfall signatures preserved in the invasive terrestrial gastropod *Lissachatina fulica*. Geochem. Geophys. Geosyst. 18 (11), 3758–3770.

Girod, A., Sassoon, D., 2022. Distribution and ecology of Zootecus insularis (Ehrenberg, 1831) (Gastropoda, Pulmonata, Achatinidae, Subulininae) and its value as a palaeoenvironmental indicator species. Basteria.

Gonfiantini, R., Stichler, W., Rozanski, K., 1995. Standards and Intercomparison Materials Distributed by the International Atomic Energy Agency for Stable Isotope Measurements (IAEA-TECDOC–825). International Atomic Energy Agency (IAEA).

Grossman, E.L., Ku, T.L., 1986. Oxygen and carbon isotope fractionation in biogenic aragonite: temperature effects. Chem. Geol.: Isotope Geosci. Sect. 59, 59–74. https://doi.org/10.1016/0168-9622(86)90057-6.

Heller, J., 1990. Longevity in molluscs. Malacologia 31 (2), 259–295.

Hoffmann, G., Rupprechter, M., Rahn, M., Preusser, F., 2015. Fluvio-lacustrine deposits reveal precipitation pattern in SE Arabia during early MIS 3. Quat. Int. 382, 145–153. https://doi.org/10.1016/j.quaint.2014.10.053.

Kieniewicz, J.M., Smith, J.R., 2007. Hydrologic and climatic implications of stable isotope and minor element analyses of authigenic calcite silts and gastropod shells from a mid-Pleistocene pluvial lake, Western Desert, Egypt. Quat. Res. 68 (3), 431–444. https://doi.org/10.1016/j.yqres.2007.07.010.

Klaus, J., McDonnell, J.J., 2013. Hydrograph separation using stable isotopes: Review and evaluation. J. Hydrol. 505, 47–64. https://doi.org/10.1016/j.jhydrol.2013.09.006.

Lécuyer, C., Marco, A.S., Lomoschitz, A., Betancort, J.F., Fourel, F., Amiot, R., Clauzel, T., Flandrois, J.-P., Meco, J., 2020. $\delta^{18}O$ and $\delta^{13}C$ of diagenetic land snail shells from the Pliocene (Zanclean) of Lanzarote, Canary Archipelago: do they still record some climatic parameters? J. Afr. Earth Sci. 162, 103702. https://doi.org/10.1016/j.jafrearsci.2019.103702.

Leng, M.J., Heaton, T.H., Lamb, H.F., Naggs, F., 1998. Carbon and oxygen isotope variations within the shell of an African land snail (*Limicolaria kambeul chudeaui* Germain): a high-resolution record of climate seasonality? The Holocene 8 (4), 407–412. https://doi.org/10.1191/095968398669296159.

Leng, M.J., Lamb, A.L., Lamb, H.F., Telford, R.J., 1999. Palaeoclimatic implications of isotopic data from modern and early Holocene shells of the freshwater snail *Melanoides tuberculata*, from lakes in the Ethiopian Rift Valley. J. Paleolimnol. 21, 97–106. https://doi.org/10.1023/a:1008079219280.

Li, Q., Dong, J., Yan, H., Huang, H., Zong, X., Wang, G., Liu, C., Cao, Y., Liu, W., An, Z., 2024. High-resolution intrashell oxygen isotope studies of Cathaica fasciola and Bradybaena ravida land snails and their environmental implications. Geophys. Res. Lett. 51 (6), e2023GL107835. https://doi.org/10.1029/2023GL107835.

Lindauer, S., 2019. Radiocarbon Reservoir Effects on Shells from SE Arabia in the Context of Paleoenvironmental Studies. Doctoral dissertation. Technical University of Darmstadt.

Lindauer, S., Marali, S., Schöne, B.R., Uerpmann, H.P., Kromer, B., Hinderer, M., 2017. Investigating the local reservoir age and stable isotopes of shells from Southeast Arabia. Radiocarbon 59 (2), 355–372. https://doi.org/10.1017/rdc.2016.80.

Lindauer, S., Milano, S., Steinhof, A., Hinderer, M., 2018. Heating mollusc shells-a radiocarbon and microstructure perspective from archaeological shells recovered from Kalba, Sharjah Emirate, UAE. J. Archaeol. Sci. Rep. 21, 528–537. https://doi.org/10.1016/j.jasrep.2018.08.041.

Long, K., Schneider, L., Williams, I.S., Fallon, S.J., Stuart-Williams, H., Haberle, S., 2020. A first look at oxygen isotope records from modern and Holocene-aged gastropod (*Stenomelania*) shells from Lake Kutubu, Papua New Guinea. J. Quat. Sci. 35 (3), 457–464. https://doi.org/10.1002/jqs.3188.

Louis, V., Besseau, L., Lartaud, F., 2022. Step in time: Biomineralisation of bivalve's shell. Front. Mar. Sci. 9, 906085. https://doi.org/10.3389/fmars.2022.906085.

Mansour, S., Darby, S., Leyland, J., Atkinson, P.M., 2021. Geospatial modelling of tropical cyclone risk along the northeast coast of Oman: Marine hazard mitigation and management policies. Mar. Policy 129, 104544.

Matter, A., Neubert, E., Preusser, F., Rosenberg, T., Al-Wagdani, K., 2015. Palaeo-environmental implications derived from lake and sabkha deposits of the southern Rub'al-Khali, Saudi Arabia and Oman. Quat. Int. 382, 120–131. https://doi.org/10.1016/j.quaint.2014.12.029.

Matter, J.M., Waber, H.N., Loew, S., Matter, A., 2006. Recharge areas and geochemical evolution of groundwater in an alluvial aquifer system in the Sultanate of Oman. Hydrogeol. J. 14, 203–224. https://doi.org/10.1007/s10040-004-0425-2.

McConnaughey, T.A., Gillikin, D.P., 2008. Carbon isotopes in mollusk shell carbonates. Geo-Mar. Lett. 28, 287–299. https://doi.org/10.1007/s00367-008-0116-4.

Milano, S., Lindauer, S., Prendergast, A.L., Hill, E.A., Hunt, C.O., Barker, G., Schöne, B.R., 2018. Mollusk carbonate thermal behaviour and its implications in understanding prehistoric fire events in shell middens. J. Archaeol. Sci. Rep. 20, 443–457. https://doi.org/10.1016/j.jasrep.2018.05.027.

Mitchell, A.J., Brandt, T.M., 2005. Temperature tolerance of red-rim melania *Melanoides tuberculatus*, an exotic aquatic snail established in the United States. Trans. Am. Fish. Soc. 134 (1), 126–131. https://doi.org/10.1577/ft03-178.1.

Mueller, D., Raith, K., Bretzke, K., Fülling, A., Parker, A.G., Parton, A., Preston, G.W., Jasim, S., Yousif, E., Preusser, F., 2023. Luminescence chronology of fluvial and aeolian deposits from the Emirate of Sharjah, UAE. Quat. Res. 112, 111–127. https://doi.org/10.1017/qua.2022.51.

Nicholson, S.L., Pike, A.W., Hosfield, R., Roberts, N., Sahy, D., Woodhead, J., Cheng, H., Lawrence Edwards, R., Affolter, S., Leuenberger, M., Burns, S.J., Matter, A., Fleitmann, D., 2020. Pluvial periods in Southern Arabia over the last 1.1 million-years. Quat. Sci. Rev. 229, 106112. https://doi.org/10.1016/j.quascirev.2019.106112.

Nizwa, 2019. Oman data weather. 2019 from the National Centre for Statistics & Informaion Sultanate of Oman. https://data.gov.om/bixytwb/weather?regions=1000000-oman (last accesses 09 February 2022).

Parker, A.G., Eckersley, L., Smith, M.M., Goudie, A.S., Stokes, S., Ward, S., White, M., Hodson, M.J., 2004. Holocene vegetation dynamics in the northeastern Rub'al-Khali desert, Arabian Peninsula: a phytolith, pollen and carbon isotope study. J. Quat. Sci. 19 (7), 665–676. https://doi.org/10.1002/jqs.880.

Parker, A.G., Preston, G.W., Parton, A., Walkington, H., Jardine, P.E., Leng, M.J., Hodson, M.J., 2016. Low-latitude Holocene hydroclimate derived from lake sediment flux and geochemistry. J. Quat. Sci. 31 (4), 286–299. https://doi.org/10.1002/jqs.2859.

Parton, A., White, T.S., Parker, A.G., Breeze, P.S., Jennings, R., Groucutt, H.S., Petraglia, M.D., 2015. Orbital-scale climate variability in Arabia as a potential motor for human dispersals. Quat. Int. 382, 82–97. https://doi.org/10.1016/j.quaint.2015.01.005.

Philippsen, B., 2013. The freshwater reservoir effect in radiocarbon dating. Herit. Sci. 1, 1–19. https://doi.org/10.1186/2050-7445-1-24.

Philippsen, B., Heinemeier, J., 2013. Freshwater reservoir effect variability in Northern Germany. Radiocarbon 55 (2–3), 1085–1101.

Prendergast, A.L., Stevens, R.E., Barker, G., O'Connell, T.C., 2015. Oxygen isotope signatures from land snail (*Helix melanostoma*) shells and body fluid: proxies for reconstructing Mediterranean and North African rainfall. Chem. Geol. 409, 87–98. https://doi.org/10.1016/j.chemgeo.2015.05.014.

Preston, G.W., Thomas, D.S., Goudie, A.S., Atkinson, O.A., Leng, M.J., Hodson, M.J., Walkington, H., Charpentier, V., Méry, S., Borgi, F., Parker, A.G., 2015. A multi-proxy analysis of the Holocene humid phase from the United Arab Emirates and its implications for Southeast Arabia's Neolithic populations. Quat. Int. 382, 277–292. https://doi.org/10.1016/j.quaint.2015.01.054.

Qamar, S.U.R., Saif, A., Altaf, J., 2017. Identification of the species of genus Zootecus on the basis of morphology. J. Biodivers. Environ. Sci. 11 (3), 122–127.

Quenu, M., Judd, E.J., Morgan-Richards, M., Trewick, S.A., Holt, K., Tyler, J., Lorrey, A. M., 2023. High-resolution stable isotope profiles from shells of the land snail *Placostylus* reveal contrasting patterns between snails originating from New Zealand and New Caledonia. J. Quat. Sci. 38 (7), 1171–1183. https://doi.org/10.1002/jqs.3536.

Raw, J.L., Perissinotto, R., Miranda, N.A.F., Peer, N., 2016. Feeding dynamics of *Melanoides tuberculata* (Müller, 1774). J. Molluscan Stud. 82 (2), 328–335. https://doi.org/10.1093/mollus/eyv070.

Ritter, A.-C., Mavromatis, V., Dietzel, M., Kwiecien, O., Wiethoff, F., Griesshaber, E., Casella, L.A., Schmahl, W.W., Koelen, J., Neuser, R.D., Leis, A., Buhl, D., Niedermayr, A., Breitenbach, S.F.M., Bernasconi, S.M., Immenhauser, A., 2017. Exploring the impact of diagenesis on (isotope) geochemical and microstructural alteration features in biogenic aragonite. Sedimentology 64 (5), 1354–1380. https://doi.org/10.1111/sed.12356.

Rosenberg, T.M., Preusser, F., Blechschmidt, I., Fleitmann, D., Jagher, R., Matter, A., 2012. Late Pleistocene palaeolake in the interior of Oman: a potential key area for the dispersal of anatomically modern humans out-of-Africa? J. Quat. Sci. 27 (1), 13–16. https://doi.org/10.1002/jqs.1560.

Rozanski, K., Araguás-Araguás, L., Gonfiantini, R., 1993. Isotopic patterns in modern global precipitation. Clim. Change Cont. Isotopic Rec. 78, 1–36. https://doi.org/10.1029/gm078p0001.

Schmitt, K.E., Walliser, E.O., Schöne, B.R., Gey, C.J., Schmidt, C., 2022. Environmental reconstructions based on aquatic and terrestrial snails originating from the early Bronze Age and the late Islamic Period–a stable isotope case study from the Al-Khashbah archaeological Site, Sultanate of Oman. J. Archaeol. Sci. Rep. 45, 103620. https://doi.org/10.1016/j.jasrep.2022.103620.

Schöne, B., Surge, D.M., 2012. Treatise online no. 46: part N, revised, volume 1, chapter 14: bivalve sclerochronology and geochemistry. Treatise. https://doi.org/10.17161/to.v0i0.4297.

Schöne, B.R., 2008. The curse of physiology—challenges and opportunities in the interpretation of geochemical data from mollusk shells. Geo-Mar. Lett. 28, 269–285. https://doi.org/10.1007/s00367-008-0114-6.

Schöne, B.R., Meret, A.E., Baier, S.M., Fiebig, J., Esper, J., McDonnell, J., Pfister, L., 2020. Freshwater pearl mussels from northern Sweden serve as long-term, high-resolution stream water isotope recorders. Hydrol. Earth Syst. Sci. 24 (2), 673–696. https://doi.org/10.5194/hess-24-673-2020.

Shanahan, T.M., Pigati, J.S., Dettman, D.L., Quade, J., 2005. Isotopic variability in the aragonite shells of freshwater gastropods living in springs with nearly constant temperature and isotopic composition. Geochim. Cosmochim. Acta 69, 3949–3966. https://doi.org/10.1016/j.gca.2005.03.049.

Sjögren, K.G., Price, T.D., 2013. A complex Neolithic economy: isotope evidence for the circulation of cattle and sheep in the TRB of western Sweden. J. Archaeol. Sci. 40 (1), 690–704. https://doi.org/10.1016/j.jas.2012.08.001.

Stott, L.D., 2002. The influence of diet on the $\delta^{13}C$ of shell carbon in the pulmonate snail *Helix aspersa*. Earth Planet. Sci. Lett. 195 (3–4), 249–259. https://doi.org/10.1016/s0012-821x(01)00585-4.

Stringer, C.A., Prendergast, A.L., 2023. Freshwater mollusc sclerochronology: trends, challenges, and future directions. Earth Sci. Rev., 104621 https://doi.org/10.1016/j.earscirev.2023.104621.

Swart, P.K., 2015. The geochemistry of carbonate diagenesis: the past, present and future. Sedimentology 62 (5), 1233–1304. https://doi.org/10.1111/sed.12205.

Taft, L., Mischke, S., Wiechert, U., Leipe, C., Rajabov, I., Riedel, F., 2014. Sclerochronological oxygen and carbon isotope ratios in Radix (Gastropoda) shells indicate changes of glacial meltwater flux and temperature since 4,200 cal yr BP at Lake Karakul, eastern Pamirs (Tajikistan). J. Paleolimnol. 52, 27–41. https://doi.org/10.1007/s10933-014-9776-4.

Taft, L., Wiechert, U., Albrecht, C., Leipe, C., Tsukamoto, S., Wilke, T., Zhang, H., Riedel, F., 2020. Intra-seasonal hydrological processes on the western Tibetan Plateau: monsoonal and convective rainfall events at~ 7.5 ka. Quat. Int. 537, 9–23. https://doi.org/10.1016/j.quaint.2020.01.027.

Terry, J., Al Ruheili, A., Boldi, R., Gienko, G., Stahl, H., 2022. Cyclone Shaheen: the exceptional tropical cyclone of October 2021 in the Gulf of Oman. Weather 77 (10), 364–370. https://doi.org/10.1002/wea.4193.

Van Rampelbergh, M., Fleitmann, D., Verheyden, S., Cheng, H., Edwards, L., De Geest, P., De Vleeschouwer, D., Burns, S.J., Matter, A., Claeys, P., Keppens, E., 2013. Mid-to late Holocene Indian Ocean Monsoon variability recorded in four speleothems from Socotra Island, Yemen. Quat. Sci. Rev. 65, 129–142.

Versteegh, E.A., Vonhof, H.B., Troelstra, S.R., Kroon, D., 2011. Can shells of freshwater mussels (Unionidae) be used to estimate low summer discharge of rivers and associated droughts? Int. J. Earth Sci. 100, 1423–1432. https://doi.org/10.1007/s00531-010-0551-0.

Wang, G., Dong, J., Han, T., Liu, C., Luo, F., Yang, H., He, M., Tang, G., Zhao, N., Zhang, Q., Xue, G., Dodson, J., Li, Q., Yan, H., 2024. Quantitative reconstruction of a single super rainstorm using daily resolved $\delta^{18}O$ of land snail shells. Sci. Bull. https://doi.org/10.1016/j.scib.2024.04.037.

Weyhenmeyer, C.E., Burns, S.J., Waber, H.N., Aeschbach-Hertig, W., Kipfer, R., Loosli, H. H., Matter, A., 2000. Cool glacial temperatures and changes in moisture source recorded in Oman groundwaters. Science 287 (5454), 842–845. https://doi.org/10.1126/science.287.5454.842.

Weyhenmeyer, C.E., Burns, S.J., Waber, H.N., Macumber, P.G., Matter, A., 2002. Isotope study of moisture sources, recharge areas, and groundwater flow paths within the eastern Batinah coastal plain, Sultanate of Oman. Water Resour. Res. 38 (10). https://doi.org/10.1029/2000WR000149, 2–1.

Woor, S., Buckland, C., Parton, A., Thomas, D.S., 2022. Assessing the robustness of geochronological records from the Arabian Peninsula: a new synthesis of the last 20 ka. Glob. Planet. Chang. 209, 103748. https://doi.org/10.1016/j.gloplacha.2022.103748.

Yanes, Y., Romanek, C.S., Delgado, A., Brant, H.A., Noakes, J.E., Alonso, M.R., Ibáñez, M., 2009. Oxygen and carbon stable isotopes of modern land snail shells as environmental indicators from a low-latitude oceanic island. Geochim. Cosmochim. Acta 73 (14), 4077–4099. https://doi.org/10.1016/j.gca.2009.04.021.

Zaarur, S., Affek, H.P., Stein, M., 2016. Last glacial-Holocene temperatures and hydrology of the Sea of Galilee and Hula Valley from clumped isotopes in *Melanopsis* shells. Geochim. Cosmochim. Acta 179, 142–155. https://doi.org/10.1016/j.gca.2015.12.034.

Zanchetta, G., Leone, G., Fallick, A.E., Bonadonna, F.P., 2005. Oxygen isotope composition of living land snail shells: data from Italy. Palaeogeogr. Palaeoclimatol. Palaeoecol. 223 (1–2), 20–33. https://doi.org/10.1016/j.palaeo.2005.03.024.